

Rethinking Large-scale Dataset Compression: Shifting Focus From Labels to Images

Lingao Xiao^{1,2,3}, Songhua Liu¹, Yang He^{1,2,3,*}, Xinchao Wang¹

¹National University of Singapore

²CFAR, Agency for Science, Technology and Research, Singapore

³IHPC, Agency for Science, Technology and Research, Singapore

{xiao_lingao, songhua.liu}@u.nus.edu,

he_yang@cfar.a-star.edu.sg, xinchao@nus.edu.sg

Abstract

Dataset distillation and dataset pruning are two prominent techniques for compressing datasets to improve computational and storage efficiency. Despite their overlapping objectives, these approaches are rarely compared directly. Even within each field, the evaluation protocols are inconsistent across various methods, which complicates fair comparisons and hinders reproducibility. Considering these limitations, we introduce in this paper a benchmark that equitably evaluates methodologies across both distillation and pruning literatures. Notably, our benchmark reveals that in the mainstream dataset distillation setting for large-scale datasets, which heavily rely on soft labels from pre-trained models, even randomly selected subsets can achieve surprisingly competitive performance. This finding suggests that an overemphasis on soft labels may be diverting attention from the intrinsic value of the image data, while also imposing additional burdens in terms of generation, storage, and application. To address these issues, we propose a new framework for dataset compression, termed *Prune, Combine, and Augment (PCA)*, which focuses on leveraging image data exclusively, relies solely on hard labels for evaluation, and achieves state-of-the-art performance in this setup. By shifting the emphasis back to the images, our benchmark and PCA framework pave the way for more balanced and accessible techniques in dataset compression research. Our code is available at: <https://github.com/ArmandXiao/Rethinking-Dataset-Compression>.

1. Introduction

Modern deep learning often relies on extensive datasets, posing challenges in computational cost and storage. Two widely adopted strategies to address these challenges are

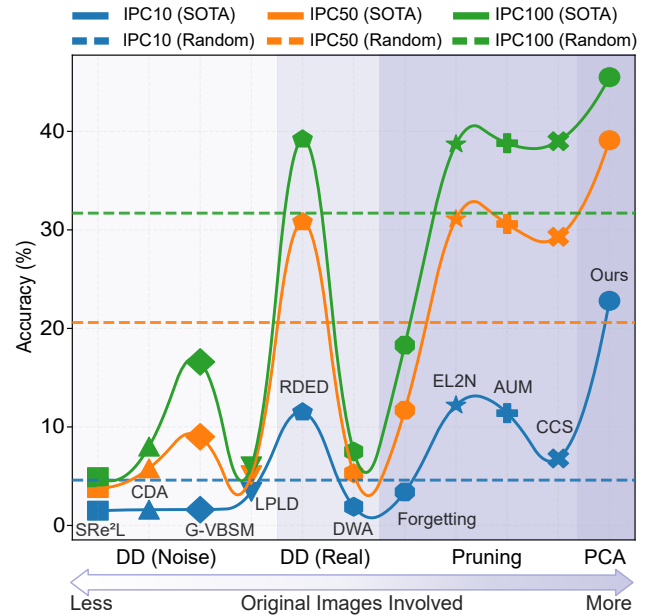


Figure 1: Benchmarking SOTA methods using **hard labels**. “DD (Noise)” and “DD (Real)” denote dataset distillation with noise and real images, respectively. Many methods struggle to outperform the random baseline, and methods utilizing more original images generally achieve better performance. Evaluation uses ResNet-18 on ImageNet-1K. Detailed data is provided in Table 5.

dataset distillation and *dataset pruning*. Dataset distillation (Yu et al., 2023) involves generating a compact set of synthetic images that encapsulate the essential attributes of the original dataset, while dataset pruning focuses on selecting the most critical subset of real images for training.

Despite sharing the same goal, these approaches are suited to different scenarios. Dataset distillation aims for significant compression ratios, often condensing down to 10 images per class (IPC), which is equivalent to $\sim 99\%$ pruning rate. In contrast, dataset pruning typically reduces dataset size by 20%-40% without significantly affecting performance. Theoretically, pruning could remove a large portion of images,

Table 1: Inconsistent evaluation settings of Dataset Distillation on ImageNet-1K. Values marked in **red** are settings different from SRe²L. † represents the IPC-dependent.

Configuration	Value	SRe ² L	CDA	RDED	G-VBSM	EDC
Epochs	300	✓	✓	✓	✓	✓
Optimizer	AdamW	✓	✓	✓	✓	✓
Model LR	0.001	✓	✓	✓	✓	✓
LR	Smooth LR	✗	✗	✓	✗	✓
LR Scheduler	CosineAnnealing	✓	✓	✓	✓	✓
Batch Size	1024	1024	128	100 [†]	1024	100
Soft Label	Single / Ensemble	Single	Single	Single	Ensemble	Ensemble
Loss Type	KL / MSE+0.1xGT	KL	KL	KL	MSE	MSE
EMA-based	✗	✗	✗	✗	✗	✓
	PatchShuffle	✗	✗	✓	✗	✓
	ResizedCrop	✓	✓	✓	✓	✓
Augmentation	CropRange	(0.08, 1)	(0.08, 1)	(0.5, 1)	(0.08, 1)	(0.5, 1)
	Flip	✓	✓	✓	✓	✓
	Cut-Mix	✓	✓	✓	✓	✓

matching the extreme compression levels of distillation. However, in such cases, the comparative effectiveness of pruning versus distillation remains uncertain. Additionally, the frameworks for evaluating pruning and distillation on large-scale datasets vary significantly.

Inconsistencies also exist within large-scale dataset distillation literature (see Table 1). Initially, SRe²L (Yin et al., 2023) employed a large batch size of 1024 for evaluation. Subsequent studies (Yin & Shen, 2024; Du et al., 2024; Sun et al., 2024) adopted much smaller batch sizes, leading to more training updates. The absence of standardized evaluation protocols regarding batch sizes and data augmentation has hampered reproducibility and made it challenging to assess new research developments.

To address these issues, we introduce a benchmark for equitable evaluation of methodologies in both dataset distillation and pruning. Our benchmark highlights a performance enhancement when using soft labels for evaluation. Randomly selected subsets equipped with soft labels show strong performance compared to SOTA methods, particularly at large IPCs (see Figure 2). Even purely random noise achieves learnable results from a pretrained teacher network using soft labels. This advantage of soft labels has shifted focus away from images to the exploitation of soft labels.

However, utilizing soft labels incurs several costs and unfairness. Firstly, soft labels are storage-intensive, often largely exceeding the storage requirements of images (Xiao & He, 2024). Secondly, the diverse storage formats of soft labels necessitate changes in dataloaders, complicating implementation as more augmentation strategies, like RandAugment in DELT (Shen et al., 2024), emerge. Lastly, soft labels introduce information beyond what is present in the compressed dataset, potentially biasing evaluations. Therefore, we further evaluate the SOTA methods without soft labels; unsurprisingly, the performance drops drastically as shown in Figure 1. For example, the performance of SRe²L drops

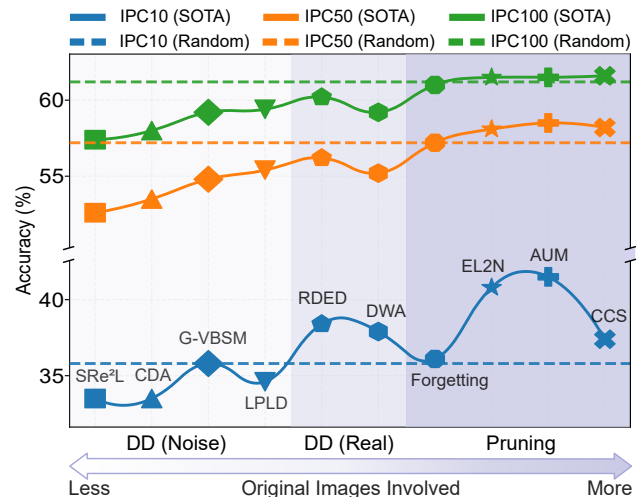


Figure 2: Benchmarking SOTA methods using **soft labels**. Many methods struggle to outperform the random baseline, particularly at large IPCs. Evaluation uses ResNet-18 on ImageNet-1K. Detailed data is provided in Table 4.

from 33.5% (with soft labels) to 1.5% (with hard labels).

To counter these challenges, we propose a hard-label-only framework, *Prune, Combine, and Augment (PCA)*, to prioritize image contributions while surpassing random baseline performance. The *PCA* framework builds on pruning insights by selecting straightforward, representative images adhering to established pruning principles, such as balanced classes and a focus on “easier” samples. These images are then compressed further and enhanced through specialized data-augmentation methods, particularly advantageous for the final small-scale datasets. Unlike conventional distillation, *PCA* does not store soft labels from pretrained models, making it viable for scenarios with constrained memory or limited access to large teacher models.

In summary, our primary contributions include:

1. A unified evaluation setting that resolves inconsistencies in previous comparisons of dataset distillation and pruning.
2. Demonstration of the importance of random baselines, revealing that many existing methods do not surpass straightforward baselines under soft-label conditions.
3. The introduction of *PCA* framework that aims to shift the focus from utilizing powerful soft labels to images themselves.
4. Extensive experiments on large-scale benchmarks, showcasing *PCA*’s consistent performance surpassing both random baselines and leading approaches across various model architectures.

2. Related Works

Dataset Distillation. Dataset distillation aims to learn compact and synthetic datasets that achieve a similar performance as the full dataset. Researchers have developed many frameworks (Wang et al., 2018; Zhao et al., 2021; Kim et al., 2022; Zhao & Bilen, 2021; Cazenavette et al., 2022; Liu et al., 2023; Lee et al., 2022; Zhao & Bilen, 2023; Wang et al., 2022; Jiang et al., 2022; Du et al., 2023; Shin et al., 2023; Deng & Russakovsky, 2022; Liu et al., 2022a; Zhao & Bilen, 2022; Wang et al., 2023; Lorraine et al., 2020; Nguyen et al., 2021a;b; Vicol et al., 2022; Zhou et al., 2022; Loo et al., 2022; Zhang et al., 2023; Cui et al., 2023; Loo et al., 2023) to effectively learn the synthetic dataset on small scale dataset like MNIST and CIFAR dataset.

However, scaling the existing framework to a large dataset suffers from unaffordable consumption in both memory and time. SRe²L (Yin et al., 2023) on the first time achieves noticeable performance by decoupling the optimization process into three phases of squeezing, recovering, and relabeling. Follow-up works (Yin & Shen, 2024; Sun et al., 2024; Du et al., 2024; Shao et al., 2024a; Loo et al., 2024) mostly focus on addressing the diversity issue of the recovery phase, with more and more attention paid to the relabeling process (Xiao & He, 2024; Zhang et al., 2024b; Qin et al., 2024b; Kang et al., 2024; Yu et al., 2025). However, most methods use different evaluation settings and lack direct comparison, and the performance of random baseline under the relabeling process is overlooked¹.

Dataset Pruning. Dataset pruning selects a representative subset by ranking images with different metrics (Coleman et al., 2020; Toneva et al., 2019; Pleiss et al., 2020; Feldman & Zhang, 2020; Paul et al., 2021). Most of the reported experiments are focused on small datasets like CIFAR or ImageNet subsets. Methods that scale to large-scale datasets focus on small or moderate pruning ratio to ensure minimum performance drop (Xia et al., 2023; Sorscher et al., 2022; Zheng et al., 2023; Zhang et al., 2024a; Grosz et al., 2024; Abbas et al., 2024). VID (Ben-Baruch et al., 2024) conducts experiments on data pruning methods using knowledge distillation. However, these experiments did not explore extreme pruning ratios, and the baselines were not compared with dataset distillation methods.

Dataset Compression. Dataset compression intuitively encompasses both dataset distillation and dataset pruning, which can work independently. Existing studies incorporate the pruning process, or coreset selection, before dataset distillation (Liu et al., 2023; Xu et al., 2025; Moser et al., 2024; Shen et al., 2024). Additionally, YOCO (He et al.,

¹We notice a concurrent work that benchmarks existing dataset distillation methods currently on small-scale datasets (i.e., CIFAR and Tiny-ImageNet), and we encourage interested readers to visit <https://github.com/NUS-HPC-AI-Lab/DD-Ranking>.

Table 2: Effect of batch size in evaluation. Results are reported using randomly sampled data in IPC-10 with ResNet-18. $A \times (B \times)$ means A is theoretical increments and B is the actual increments.

Batch Size \uparrow	Performance \downarrow	Memory Requirement \uparrow	Training Time \downarrow
32	37.7 \pm 0.4 %	1 \times	32 \times (26 \times)
128	35.8 \pm 0.1 %	4 \times (3 \times)	8 \times (7 \times)
1024	23.7 \pm 0.1 %	32 \times (17 \times)	1 \times

Table 3: Random Baseline with Soft Label Distillation.

IPC/BS	ResNet-18			ResNet-50		ResNet-101
	32	128	1024	32	128	128
1	4.1 \pm 0.2	4.3 \pm 0.1	1.9 \pm 0.1	3.7 \pm 0.2	3.6 \pm 0.1	3.1 \pm 0.5
10	37.7 \pm 0.4	35.8 \pm 0.2	23.6 \pm 0.3	42.9 \pm 0.6	39.3 \pm 1.6	37.7 \pm 1.3
20	49.6 \pm 0.7	48.5 \pm 0.1	38.2 \pm 0.3	54.8 \pm 0.6	55.5 \pm 0.2	52.9 \pm 3.0
50	58.0 \pm 0.1	57.2 \pm 0.2	52.4 \pm 0.2	64.3 \pm 0.2	64.2 \pm 0.1	62.1 \pm 2.2
100	61.5 \pm 0.1	61.2 \pm 0.2	58.3 \pm 0.0	67.4 \pm 0.1	67.0 \pm 0.2	65.8 \pm 0.9
200	64.9 \pm 0.5	64.2 \pm 0.1	61.6 \pm 0.0	68.6 \pm 0.2	68.8 \pm 0.1	69.1 \pm 0.1

2024) examines the pruning rules specifically for distilled datasets. However, given the distinctly different nature and settings of these two tasks, it remains unclear which method represents the state-of-the-art (SOTA) in the field of data compression today. This lack of direct comparison may lead to misunderstandings about the data compression task and result in ineffective combinations of methods.

3. Benchmarking Data Compression

Inconsistent Evaluation Settings in Dataset Distillation.

As illustrated in Table 1, the domain of large-scale dataset distillation does not have a consistent evaluation setting. Using different settings does not mean wrong; however, it may lead to unfair comparison and potentially hinder both readers and researchers from understanding how important the proposed method is and where the improvement comes from. Among these configurations, the most important one is the different batch sizes. Using a different batch size largely affects performance, memory requirements, and training efficiency, as shown in Table 2. In the following paper, we use CDA’s setting (Yin & Shen, 2024) as the **standard evaluation setting** since they only change the batch size from the initial implementation while providing a good performance and efficiency trade-off.

Undervalued Random Baseline with Distillation Training.

Many existing works (Yin et al., 2023; Yin & Shen, 2024; Sun et al., 2024; Xiao & He, 2024) fail to recognize the value of random baselines. By evaluating the random dataset under the standard evaluation setting, we notice that most works fail to surpass the random baseline (see Fig. 2 and Table 3), creating a huge gap in understanding the task of large-scale dataset distillation. Especially, the gap becomes more distinguished as IPC scales.

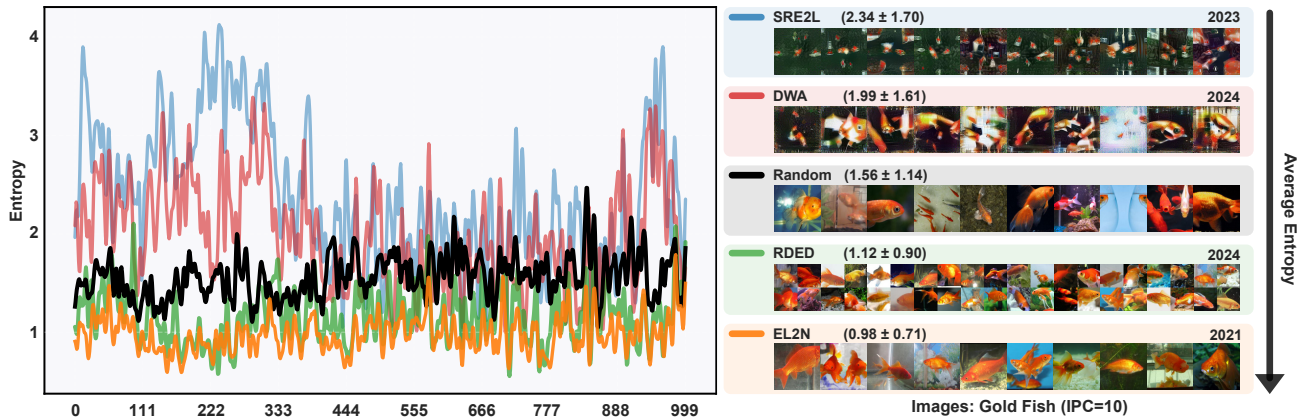


Figure 3: Entropy analysis of different datasets with IPC=10. Images are randomly sampled from the corresponding dataset for visualization. The classifier used for entropy analysis is the pretrained EfficientNet-B0 (Tan & Le, 2019).

Understanding Effect of Images and Soft Labels. To evaluate the effectiveness of images, Figure 2 offers valuable insights into both the quantity and quality of original images used, which may significantly affect performance. The subpar results of earlier dataset distillation methods compared to random baselines suggest that **image distortion, learned during the dataset distillation process, adversely impacts performance**. Furthermore, when using **purely noisy images**, the student network can successfully learn to replicate the outputs of a pretrained teacher model, as demonstrated in Appendix D.1. This suggests that soft labels derived from the teacher model provide sufficient information for the student to learn even from random noise, thereby reducing the distinctive impact of the images.

Reducing Size of Pre-Generated Soft Labels. By utilizing distillation training, distilled datasets deliver an extraordinary performance against early exploration on large-scale dataset distillation (Cui et al., 2023). However, a critical question arises: *Does using distillation training for evaluation align with the motivation and practical needs of dataset compression?* Requiring a pretrained model to aid the training with a compressed dataset essentially reduces the practical value of the compressed dataset. One scenario that makes the task valid is when the pretrained model is not available during deployment but during development. One workaround is to store all pre-generated soft labels locally.

Problems of Pre-Generated Soft Labels. However, as mentioned by Xiao & He and Qin et al., the soft label storage far exceeds the image storage. For example, the label storage of ImageNet-21K-P IPC20 is over 1.2 TB, while the images are merely 5 GB. Existing methods (Xiao & He, 2024; Zhang et al., 2024b) have started to reduce soft label storage, but pre-generated soft labels still face several disadvantages. (1) Soft labels are stored in a very different format from images, and special changes to the dataloader are required;

(2) using soft labels during training creates additional system I/O costs besides soft label generation. Last but not least, as more and more data augmentation is introduced; (3) the use of soft labels becomes increasingly complicated as more advanced augmentation (i.e., RandAugment; Shen et al. 2024) is introduced; (4) soft label introduces knowledge beyond the compressed datasets, potentially biasing the evaluation results.

We believe that, in the field of large-scale dataset distillation, efforts should be focused on enhancing the quality of distilled images rather than prioritizing further exploitation of soft labels. Consequently, the preferred approach should be controlling the size of soft labels or even transitioning to using only hard labels.

4. Framework: Prune, Combine, and Augment

We introduce a novel framework, termed *Prune, Combine, and Augment (PCA)*, which utilizes only hard labels during deployment and evaluation. This framework aims to enhance the understanding of dataset compression methods by showcasing their true contributions.

4.1. Prune Dataset

Relying solely on hard labels for evaluation allows us to leverage key insights from dataset pruning: (1) **Class balance becomes increasingly important as the dataset size diminishes** (He et al., 2024), and (2) **Simpler images are preferred when the dataset size is small** (Sorscher et al., 2022; Zheng et al., 2023; He et al., 2024).

Common Images-per-class (IPC) in dataset distillation reflects high pruning ratios, necessitating methods to align with pruning guidelines. We analyze the patterns generated by dataset distillation images to verify if they meet these

criteria. First, dataset distillation naturally achieves class balance using IPC, ensuring perfect class balance. Second, Figure 3 provides an intuitive entropy analysis, and we can gauge the dataset’s complexity by extending the use of entropy as a measure of uncertainty (Coleman et al., 2020; Sun et al., 2024). A dataset with high average entropy is deemed relatively challenging. In addition, we can visually compare images compressed by different methodologies in Figure 3.

Consequently, we propose to select images according to pruning metrics while adhering to the pruning rules (He et al., 2024). Specifically, we use the reverse metric of EL2N (Paul et al., 2021), meanwhile forcing strict class balance. This approach is optimization-free that requires no pretrained model for evaluation.

4.2. Combine Images

RDED (Sun et al., 2024) combines image patches that are selected from random crops. We contend that the selection of these cropped patches may not always lead to performance improvements. In Section 4.2.1, we provide a theoretical examination of the cropping operation. Further elaboration on our method of image combination is presented in Section 4.2.2.

4.2.1. THEORETICAL ANALYSIS ON CROPPING

In Proposition 4.1, we explore in detail why the metric employed by RDED (Sun et al., 2024) fails to be universally applicable. We compare it with the metric utilized in the pruning literature (Coleman et al., 2020) to highlight these differences. Subsequently, in Theorem 4.2, we demonstrate why utilizing a pretrained model to directly rank the cropped image patches is inappropriate, and the cropped dataset may not bring performance improvement as it does not consider training time augmentation.

Proposition 4.1 (proof in Appendix A.2). *Let $\mathcal{D} = \{x_i\}_{i=1}^N$ be a dataset of images, and let P_θ be a probabilistic model parameterized by θ . Lowering $\text{NLL}(\mathcal{D}; \theta)$ through a selective cropping operation \mathcal{C} (Sun et al., 2024), resulting in a new dataset $\mathcal{D}' = \mathcal{C}(\mathcal{D})$, does **not** necessarily reduce the entropy $H(\mathcal{D}')$ of the dataset:*

$$\text{NLL}(\mathcal{D}'; \theta) < \text{NLL}(\mathcal{D}; \theta) \not\Rightarrow H(\mathcal{D}') < H(\mathcal{D}).$$

Theorem 4.2 (proof in Appendix A.3). *Let \mathcal{D} be a dataset and let $\mathcal{D}' = \mathcal{C}(\mathcal{D})$ be a selectively cropped version such that $H(\mathcal{D}') < H(\mathcal{D})$. Let p_θ be a model pretrained on \mathcal{D} using an augmentation strategy \mathcal{A} that includes random cropping operations. Then, the entropy evaluated by the model on \mathcal{D}' , denoted as $H_{p_\theta}(\mathcal{D}')$, does not directly reflect the image quality of \mathcal{D}' . Specifically, under certain conditions, the following inequalities hold:*

$$H_{p_\theta}(\mathcal{A}(\mathcal{D}')) \geq H_{p_\theta}(\mathcal{A}(\mathcal{D})),$$

$$\mathcal{P}(\mathcal{A}(\mathcal{D}')) \leq \mathcal{P}(\mathcal{A}(\mathcal{D})),$$

where \mathcal{P} denotes the model performance metric.

4.2.2. COMBINING IMAGES WITHOUT CROPPING

To further condense the “essence”, using a composite pattern of images (e.g., combining multiple images into one; Kim et al. 2022; Sun et al. 2024) condenses information of multiple images into a single one with no significant information loss on the diversity and richness of the dataset. However, given that our images are carefully selected due to pruning rules, the necessity of patch selection proposed on randomly selected images (Sun et al., 2024) warrants reevaluation. Instead of randomly cropping patches and assessing each patch’s quality, retaining complete images, which hold the majority of information, is preferable as each selected image values. Since the cropping operation (i.e., patch selection) is irreversible, we only leverage cropping during training to ensure information is recoverable.

A fundamental distinction between dataset pruning and distillation is the modification state of original images. Unlike dataset distillation/condensation, where pixel modifications occur, our approach creates a composite image by combining entire images. This “combined” methodology is an intermediary approach, utilizing unmodified imagery to construct new samples.

4.3. Scaling-Law-Aware Augmentation

Scaling-law usually refers to scaling up the model (Kaplan et al., 2020); however, we refer to the scaling-law of the dataset (Sorscher et al., 2022), especially when scaling down. After acquiring a small-scale dataset, it remains crucial to unveil its potential and effectively harness the available information. Augmentation typically serves as the tool to achieve this, but it is imperative that these techniques are harmoniously integrated with the dataset’s intrinsic properties, ensuring alignment with pruning principles. For example, RDED (Sun et al., 2024) introduces “patch shuffling” to enhance the dataset’s diversity. However, during training, the Random Resized Crop operation, when directly applied to the combined image, can inadvertently transform simpler images into more complex ones, thereby violating the pruning rule.

To counteract this issue, we propose a *patch extraction* strategy, which involves opting for random patch selection rather than shuffling, as depicted in the lower branch of Figure 4. This approach selects a single image patch for subsequent augmentation, with the image resolution being interpolated using the *RandomResizedCrop* technique. This differs from IDC’s approach (Kim et al., 2022), which decodes a single combined image into multiple images. In contrast, random patch extraction confines the cropping scope to within a

Table 4: Benchmarking SOTA methods against random baseline under evaluation with **soft labels**. † means optimization-free distillation approaches. ResNet-18 on ImageNet-1K. Table with standard deviation is provided in Appendix C.1.

IPC	Random	SRe ² L	DD with Noise Initialization			LPLD	DD with Real Initialization		Pruning Method with Rules			
			CDA	G-VBSM	RDED [†]		DWA	Forgetting	EL2N	AUM	CCS	
10	35.8±0.2	33.5↓2.3	33.5↓2.3	35.8=0.0	34.6↓1.2	38.4↑2.6	37.9↑2.1	36.1↑0.3	40.8↑5.0	41.5↑5.7	37.4↑1.6	
50	57.2±0.2	52.6↓4.6	53.5↓3.7	54.8↓2.4	55.4↓1.8	56.2↓1.0	55.2↓2.0	57.2=0.0	58.1↑0.9	58.5↑1.3	58.2↑1.0	
100	61.2±0.2	57.4↓3.8	58.0↓3.2	59.2↓2.0	59.4↓1.8	60.2↓1.0	59.2↓2.0	61.0↓0.2	61.5↑0.3	61.5↑0.3	61.6↑0.4	

Table 5: Benchmarking SOTA methods against random baseline under evaluation with **hard labels**. † means optimization-free distillation approaches. ResNet-18 on ImageNet-1K. Table with standard deviation is provided in Appendix C.2.

IPC	Random	DD with Noise Initialization				DD with Real Initialization		Pruning Method with Rules				PCA Framework
		SRe ² L	CDA	G-VBSM	LPLD	RDED [†]	DWA	Forgetting	EL2N	AUM	CCS	Ours
10	4.6±0.1	1.5↓3.1	1.6↓3.0	1.6↓3.0	3.4↓1.2	11.5↑6.9	1.9↓2.7	3.4↓1.2	12.2↑7.6	11.4↑6.8	6.8↑2.2	22.8↑18.2
50	20.6±0.1	3.8↓16.8	5.8↓14.8	9.0↓11.6	5.1↓15.5	30.8↑10.2	5.3↓15.3	11.7↓8.9	31.1↑10.5	30.6↑10.0	29.3↑8.7	39.1↑18.5
100	31.7±0.6	4.9↓26.8	8.0↓23.7	16.6↓15.1	6.0↓25.7	39.2↑7.5	7.5↓24.2	18.3↓13.4	38.7↑7.0	38.8↑7.1	39.0↑7.3	45.5↑13.8

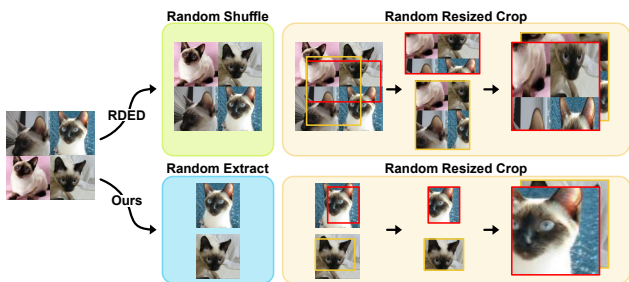


Figure 4: Patch Shuffling vs. Patch Extraction.

single patch, thereby effectively limiting the cropping area without introducing significant training overhead.

We emphasize the importance of using an effective augmentation strategy. When dealing with a small number of images, achieving good performance can be challenging. A well-crafted augmentation method can greatly enhance the potential of the images. Furthermore, the augmentation process should be aware of scaling laws, as most pruning scores are derived from training that includes data augmentation.

5. Experiment

5.1. Experiment Settings

All experiments are conducted on ImageNet-1K using CDA’s evaluation settings (see Table 1) unless otherwise indicated. Additional settings, including dataset, networks, and baseline specifications, can be found in Appendix B.

5.2. Primary Results

Benchmarking SOTA methods with Soft Labels. Beforehand, it is very hard to directly compare the results and effectiveness of dataset distillation methods and pruning methods due to a (1) **completely evaluation setting** and (2) **large discrepancy in pruning ratios**. Table 4 benchmarks

Table 6: Performance of pruning methods at extreme pruning ratio. The best setting is marked in **bold**, and the best method is marked in underline.

Setting	Method	IPC10 (99.22%)				IPC50 (96.97%)			
		hard	hard _B	easy	easy _B	hard	hard _B	easy	easy _B
Soft Label	Forgetting	25.9	32.9	6.1	36.1	53.0	56.7	52.3	57.2
	AUM	27.1	37.4	12.2	41.5	53.7	56.8	45.3	58.5
	EL2N	28.7	36.0	14.2	40.8	54.4	56.9	46.0	58.1
Hard Label	Forgetting	0.4	4.4	0.1	3.4	15.3	21.7	0.3	11.6
	AUM	0.2	1.4	0.1	11.4	1.8	4.4	0.3	30.6
	EL2N	0.2	1.4	0.2	12.2	3.2	4.2	0.3	31.1

existing dataset distillation methods and dataset pruning methods under the same evaluation setting. We categorize existing data compression methods into three main categories: (1) dataset distillation with random noise as initialization, (2) dataset distillation with randomly sampled real images as image initialization, and (3) dataset pruning adhering to the pruning rules or scaling laws. We notice that by increasing the batch size in the evaluation setting, the performance SRe²L (Yin et al., 2023) catches up with other SOTA methods (Yin & Shen, 2024; Xiao & He, 2024). However, with this being said, many SOTA methods cannot beat the random baseline. In addition, by using real images as initialization, the diversity problem that many works (Shen et al., 2024; Yin & Shen, 2024; Xiao & He, 2024; Sun et al., 2024; Du et al., 2024) are targeting is addressed. Surprisingly, pruning methods that are published 3-5 years ago (Toneva et al., 2019; Pleiss et al., 2020; Paul et al., 2021) unanimously outperform random baselines, and it’s time to call attention to this under-explored topic. As a result, an interesting observation is that the performance improves as the images include more prior knowledge of original datasets.

Benchmarking SOTA methods with Hard Labels. Table 5 evaluates the SOTA methods in a more recommendable ap-

Table 7: Ablation study of the proposed PCA framework. AdamW (0.01) means AdamW optimizer with an initial learning rate of 0.01. + denotes add-on components, and → denotes a choice from A or B. Based results are in **bold**. ResNet-18 on ImageNet-1K.

Ablation	Method	10	50	100
AdamW (0.01)	Random	4.6	21.2	31.4
	+ Pruning	12.2 ^{↑7.6}	31.1 ^{↑10.5}	38.8 ^{↑7.1}
	+ Combine	14.4 ^{↑9.8}	32.4 ^{↑11.8}	39.4 ^{↑7.7}
	+ Augment	22.8^{↑18.2}	39.1^{↑17.9}	45.5^{↑14.1}
	RDED	11.5 ^{↑6.9}	30.8 ^{↑10.2}	39.2 ^{↑7.5}
SGD (0.1)	→ Augment (Shuffle)	12.9 ^{↑8.3}	32.8 ^{↑12.2}	41.4 ^{↑9.7}
	→ Augment (Extract)	19.2 ^{↑14.6}	37.7 ^{↑17.1}	44.2 ^{↑12.5}
	Random	5.1	26.6	38.9
	RDED (+ Extract)	22.2 ^{↑17.1}	42.0 ^{↑15.4}	47.6 ^{↑8.7}
	Ours	25.6^{↑20.5}	42.1^{↑15.5}	48.6^{↑9.7}

proach that does not introduce any additional storage costs besides the images or requires pretrained knowledge. By utilizing only the hard labels, most of the results were based on soft label benchmarks, besides forgetting metrics. In addition, the PCA (Prune, Combine, and Augment) framework essentially exceeds the random baseline and other SOTA methods at all tested IPCs.

Sanity Check on Pruning Rules and Scaling Laws. Previous pruning methods have made the conclusion that when the dataset is small, (1) easy images are preferred, and (2) class balance is important. However, the previous settings do not entirely fit the current scenario. For example, previous dataset pruning works (Zheng et al., 2023) do not go to extreme pruning ratios such as IPC10, equivalent to $1 - (10 * 1000 / 1, 281, 167) = 99.2\%$ pruning rate, and He et al. conducts pruning on distilled datasets. Therefore, experiments are conducted to verify if the previous rules still work in extreme cases with real images. Table 6 shows that the two rules hold even if the pruning ratio is extremely high on original datasets. For example, from evaluation under both soft label settings and hard label settings, we can conclude that selecting easy images with balanced classes delivers the best results. Moreover, EL2N (Paul et al., 2021) shows superior performance and requires less time for ranking, so we use it as our pruning method. Analysis of reasons why Forgetting (Toneva et al., 2019) performs worse is provided in Appendix D.4.

5.3. More Experiments

Ablation Study. Table 7 demonstrates the improvements contributed by each component under hard-label-only settings. Among the components – Pruning, Combine, and Augment – augmentation (specifically, patch extraction) proves to be the most impactful. It is important to note that this augmentation is tailored specifically for combined images and can be directly applied to RDED (Sun et al., 2024). To provide further insight, we have included an ab-

Table 8: Cross-architecture performance of PCA framework (hard-label) with IPC10, IPC50, and IPC100 on ImageNet-1K. “→ SGD” denotes evaluation with SGD setting.

Model	Params.	Full Acc.	10	50	100
ResNet-18 (He et al., 2016)	11.7 M	69.76	22.8	39.1	45.5
→ SGD			25.6	42.1	48.6
ResNet-50 (He et al., 2016)	25.6 M	76.13	23.0	42.3	48.3
→ SGD			25.3	43.2	50.5
ResNet-101 (He et al., 2016)	44.5 M	77.37	25.8	42.7	49.6
→ SGD			25.9	46.3	53.6
MobileNet-V2 (Sandler et al., 2018)	3.5 M	71.88	21.9	39.1	45.3
EfficientNet-B0 (Tan & Le, 2019)	5.3 M	77.69	25.0	42.4	50.4
Swin-V2-Tiny (Liu et al., 2022b)	28.4 M	82.07	15.3	37.8	48.2

Table 9: Hard label performance against soft labels. ResNet-18, ImageNet-1K. Baseline data taken from Xiao & He. * denotes using SGD setting.

Label Compression Rate	30× SRe ² L	40× CDA	100× LPLD	> 300× PCA*
IPC10	14.1	13.2	9.6	25.6
IPC50	37.2	38.0	33.7	42.4
IPC100	46.7	47.2	44.7	48.8

lation study that explicitly compares the previously used augmentation method, Patch Shuffling, with our proposed Patch Extraction. The results clearly indicate that patch extraction offers significant advantages over patch shuffling. Additionally, since the evaluation settings for pruning methods use SGD with an initial learning rate of 0.1, we have also conducted evaluations under this configuration. Our observations reveal that even random baselines benefit from using SGD (0.1), showing a distinct advantage over AdamW (0.01). Nevertheless, in all cases, the proposed PCA framework yields significant improvements.

Cross Architecture Performance. Table 8 demonstrates a good generalization ability of the proposed framework. For all validation models, the performance scales well with the dataset size. In addition, the framework scales well with improved model capacity, with one exception on the transformer-based Swin-V2-Tiny model (Liu et al., 2022b). Since the transformer-based model is extremely data-hungry, a trend is also observed in previous works (Xiao & He, 2024; Sun et al., 2024).

Performance Against Soft Labels. Despite having inevitable drawbacks and unfairness as mentioned in Section 3, the cumbersome storage of soft labels can be addressed in some degree. Table 9 shows our hard-label-only framework can perform on par or even surpass previous methods using part of soft labels. In theory, the maximum soft label compression rate is limited to 300× in ImageNet-1K setting, as each image requires a soft label per epoch for 300 epochs. Since we do not use soft labels at all, our soft label

Table 10: Dataset cropping.

Observer	Metric	$N = 5$	$N = 20$
		EfficientNet-B0	NLL
	Entropy	17.2	18.1
ResNet	NLL	18.7	17.1
	Entropy	18.0	18.3
No Crop		22.8	

 Table 11: Crop ratio (r) during training.

range:=(r , 1.0)	IPC10	IPC50
$r = 0.01$	22.1	39.0
$r = 0.08$	22.8	39.1
$r = 0.5$	22.2	38.6
$r = 0.8$	21.0	35.5
$r = 1.0$	18.7	34.0

Table 12: Experiments with regularization-based data augmentation of Ours PCA framework in the SGD setting. ‘‘Crop’’ refers to *RandomResizedCrop* with cropping range in (0.08, 1.00). The ‘‘Mix Probability’’ refers to the likelihood of performing data mixing, where a value of 1.0 indicates that data mixing is always conducted. Experiments are conducted on ResNet-18, IPC10 of ImageNet-1K.

Crop	Data Mixing	Label Mixing	Mix Probability		
			0.2	0.5	1.0
✓	✗	-	25.6		
✓	CutMix	✓	23.8 \downarrow 1.8	23.0 \downarrow 2.6	17.4 \downarrow 8.2
		✗	25.5 \downarrow 0.1	24.7 \downarrow 0.9	23.0 \downarrow 2.6
✓	Mixup	✓	25.7 \uparrow 0.1	23.0 \downarrow 2.6	7.7 \downarrow 17.9
		✗	25.9 \uparrow 0.3	25.1 \downarrow 0.5	17.6 \downarrow 8.0
✓	Cutout	-	26.2 \uparrow 0.6	25.7 \uparrow 0.1	25.3 \downarrow 0.3

compression rate is $> 300\times$.

Effect of Cropping. In addition to the theoretical analysis (Section 4.2.1) of the effects of cropping, we conducted experiments to validate our findings. It is important to note that cropping can be performed both before and during training. We refer to cropping the dataset before training a model as dataset cropping, which is irreversible. Table 10 shows that regardless of the metric and observer used to select patches from a well-pruned dataset, dataset cropping negatively impacts performance. This behavior can be explained by Theorem 4.2. Another cropping operation occurs during training augmentation (specifically, *RandomResizedCrop*), which is ‘‘recoverable’’ because the original image remains unchanged, and the cropping operation in each epoch is independent. Table 11 presents performance under different training crop ratios.

Regularization-based Data Augmentation. In addition to common augmentation techniques such as random resized crop and horizontal flips, data mixing augmentation (i.e., Mixup, Cutout, and CutMix) is regularization-based data augmentation that reduces overfitting by providing diverse and challenging examples during training. Among regularization-based augmentation techniques, Table 12 shows Cutout demonstrates the best performance, achieving consistent accuracy levels of 26.2%, 25.7%, and 25.3% with *RandomResizedCrop*. This performance is attributed to being best aligned with scaling law: first, Cutout preserves label integrity by avoiding label mixing, which is particu-



Figure 5: Randomly sampled PCA images.

larly advantageous in scenarios with limited data. Second, the augmentations are applied to individual images without cross-sample interactions, thereby maintaining sample simplicity. In contrast, techniques such as CutMix and Mixup exhibit notable performance degradation with increasing mixing probabilities, especially in the presence of label mixing. More analysis is provided in Appendix D.3.

Additional Experiments. Additional experiments and analysis are provided in Appendix D, including SRe²L with real images as initialization (Appendix D.2), the relationship between data balance and data stratification (Appendix D.5), PCA with different pruning methods (Appendix D.6), discussion of Mosaic Augmentation (Appendix D.7), and computation cost analysis (Appendix D.8).

Visualization. Figure 5 presents our compressed datasets, more visualization including baseline methods are provided in Appendix E.

6. Conclusion, Limitation, and Future Work

In this paper, we demonstrated that dataset compression can significantly reduce computational and storage overhead in large-scale machine learning tasks without severely compromising performance. By unifying evaluation settings for both dataset distillation and pruning, we established a fair ground for comparing these two lines of research. Our proposed *Prune, Combine, and Augment (PCA)* framework capitalizes on pruning-based metrics to select representative images, merges them in a way that preserves core data characteristics, and applies carefully designed augmentation to counteract overfitting issues. Unlike soft-label distillation approaches that often rely on extensive pretrained resources, PCA employs purely hard-label supervision, thereby lowering both memory and complexity requirements. Extensive experimental results illustrated the capacity of PCA to outperform conventional baselines and existing SOTA methods, especially at extreme compression ratios.

Limitations and future works are discussed in Appendix F and Appendix G, respectively.

Impact Statement

This paper addresses pressing challenges in dataset compression by establishing a benchmark for fair comparison across dataset distillation and pruning techniques. By highlighting inconsistencies in previous evaluations, we draw attention to the need for standardized practices that enhance reproducibility and fairness. Our proposed *Prune, Combine, and Augment (PCA)* framework prioritizes image data and utilizes only hard labels, thereby reducing storage and computational demands traditionally associated with soft labels. This approach not only makes dataset compression more practical and accessible but also shifts the research focus back to the images themselves, potentially leading to more balanced and efficient methods. Through these efforts, we aim to foster responsible advancements in large-scale machine learning while ensuring the benefits are accessible to a wider range of practitioners.

References

- Abbas, A. K. M., Rusak, E., Tirumala, K., Brendel, W., Chaudhuri, K., and Morcos, A. S. Effective pruning of web-scale datasets based on complexity of concept clusters. In *Proc. Int. Conf. Learn. Represent.*, 2024.
- Ben-Baruch, E., Botach, A., Kviatkovsky, I., Aggarwal, M., and Medioni, G. Distilling the knowledge in data pruning. *arXiv preprint arXiv:2403.07854*, 2024.
- Bochkovskiy, A., Wang, C.-Y., and Liao, H.-Y. M. Yolov4: Optimal speed and accuracy of object detection. *arXiv preprint arXiv:2004.10934*, 2020.
- Cazenavette, G., Wang, T., Torralba, A., Efros, A. A., and Zhu, J.-Y. Dataset distillation by matching training trajectories. In *Proc. IEEE Conf. Comput. Vis. Pattern Recog.*, 2022.
- Coleman, C., Yeh, C., Mussmann, S., Mirzasoleiman, B., Bailis, P., Liang, P., Leskovec, J., and Zaharia, M. Selection via proxy: Efficient data selection for deep learning. In *Proc. Int. Conf. Learn. Represent.*, 2020.
- Cui, J., Wang, R., Si, S., and Hsieh, C.-J. Scaling up dataset distillation to imagenet-1k with constant memory. In *Proc. Int. Conf. Mach. Learn.*, pp. 6565–6590. PMLR, 2023.
- Deng, J., Dong, W., Socher, R., Li, L.-J., Li, K., and Fei-Fei, L. Imagenet: A large-scale hierarchical image database. In *Proc. IEEE Conf. Comput. Vis. Pattern Recog.*, pp. 248–255. Ieee, 2009.
- Deng, Z. and Russakovsky, O. Remember the past: Distilling datasets into addressable memories for neural networks. In *Proc. Adv. Neural Inform. Process. Syst.*, 2022.
- DeVries, T. and Taylor, G. W. Improved regularization of convolutional neural networks with cutout. *arXiv preprint arXiv:1708.04552*, 2017.
- Du, J., Jiang, Y., Tan, V. T., Zhou, J. T., and Li, H. Minimizing the accumulated trajectory error to improve dataset distillation. In *Proc. IEEE Conf. Comput. Vis. Pattern Recog.*, 2023.
- Du, J., Zhang, X., Hu, J., Huang, W., and Zhou, J. T. Diversity-driven synthesis: Enhancing dataset distillation through directed weight adjustment. In *Proc. Adv. Neural Inform. Process. Syst.*, 2024.
- Feldman, V. and Zhang, C. What neural networks memorize and why: Discovering the long tail via influence estimation. In *Proc. Adv. Neural Inform. Process. Syst.*, pp. 2881–2891, 2020.
- Grosz, S., Zhao, R., Ranjan, R., Wang, H., Aggarwal, M., Medioni, G., and Jain, A. Data pruning via separability, integrity, and model uncertainty-aware importance sampling. In *International Conference on Pattern Recognition*, pp. 398–413. Springer, 2024.
- He, K., Zhang, X., Ren, S., and Sun, J. Deep residual learning for image recognition. In *Proc. IEEE Conf. Comput. Vis. Pattern Recog.*, pp. 770–778, 2016.
- He, Y., Xiao, L., and Zhou, J. T. You only condense once: Two rules for pruning condensed datasets. In *Proc. Adv. Neural Inform. Process. Syst.*, 2024.
- Jiang, Z., Gu, J., Liu, M., and Pan, D. Z. Delving into effective gradient matching for dataset condensation. *arXiv preprint arXiv:2208.00311*, 2022.
- Kang, S., Lim, Y., and Shim, H. Label-augmented dataset distillation. *arXiv preprint arXiv:2409.16239*, 2024.
- Kaplan, J., McCandlish, S., Henighan, T., Brown, T. B., Chess, B., Child, R., Gray, S., Radford, A., Wu, J., and Amodei, D. Scaling laws for neural language models. *arXiv preprint arXiv:2001.08361*, 2020.
- Kim, J.-H., Kim, J., Oh, S. J., Yun, S., Song, H., Jeong, J., Ha, J.-W., and Song, H. O. Dataset condensation via efficient synthetic-data parameterization. In *Proc. Int. Conf. Mach. Learn.*, 2022. URL <https://github.com/snu-mlab/Efficient-Dataset-Condensation>.
- Lee, H. B., Lee, D. B., and Hwang, S. J. Dataset condensation with latent space knowledge factorization and sharing. *arXiv preprint arXiv:2208.10494*, 2022.
- Liu, S., Wang, K., Yang, X., Ye, J., and Wang, X. Dataset distillation via factorization. In *Proc. Adv. Neural Inform. Process. Syst.*, 2022a.

- Liu, Y., Gu, J., Wang, K., Zhu, Z., Jiang, W., and You, Y. DREAM: Efficient dataset distillation by representative matching. *arXiv preprint arXiv:2302.14416*, 2023.
- Liu, Z., Hu, H., Lin, Y., Yao, Z., Xie, Z., Wei, Y., Ning, J., Cao, Y., Zhang, Z., Dong, L., et al. Swin transformer v2: Scaling up capacity and resolution. In *Proceedings of the IEEE/CVF conference on computer vision and pattern recognition*, pp. 12009–12019, 2022b.
- Loo, N., Hasani, R., Amini, A., and Rus, D. Efficient dataset distillation using random feature approximation. In *Proc. Adv. Neural Inform. Process. Syst.*, 2022.
- Loo, N., Hasani, R., Lechner, M., and Rus, D. Dataset distillation with convexified implicit gradients. In *Proc. Int. Conf. Mach. Learn.*, 2023.
- Loo, N., Maalouf, A., Hasani, R., Lechner, M., Amini, A., and Rus, D. Large scale dataset distillation with domain shift. In *Proc. Int. Conf. Mach. Learn.*, 2024.
- Lorraine, J., Vicol, P., and Duvenaud, D. Optimizing millions of hyperparameters by implicit differentiation. In *International Conference on Artificial Intelligence and Statistics*, pp. 1540–1552, 2020.
- Moser, B. B., Raue, F., Nauen, T. C., Frolov, S., and Dengel, A. Distill the best, ignore the rest: Improving dataset distillation with loss-value-based pruning. *arXiv preprint arXiv:2411.12115*, 2024.
- Nguyen, T., Chen, Z., and Lee, J. Dataset meta-learning from kernel ridge-regression. In *Proc. Int. Conf. Learn. Represent.*, 2021a.
- Nguyen, T., Novak, R., Xiao, L., and Lee, J. Dataset distillation with infinitely wide convolutional networks. In *Proc. Adv. Neural Inform. Process. Syst.*, pp. 5186–5198, 2021b.
- Paul, M., Ganguli, S., and Dziugaite, G. K. Deep learning on a data diet: Finding important examples early in training. In *Proc. Adv. Neural Inform. Process. Syst.*, pp. 20596–20607, 2021.
- Pleiss, G., Zhang, T., Elenberg, E., and Weinberger, K. Q. Identifying mislabeled data using the area under the margin ranking. In *Proc. Adv. Neural Inform. Process. Syst.*, pp. 17044–17056, 2020.
- Qin, T., Deng, Z., and Alvarez-Melis, D. Distributional dataset distillation with subtask decomposition. *arXiv preprint arXiv:2403.00999*, 2024a.
- Qin, T., Deng, Z., and Alvarez-Melis, D. A label is worth a thousand images in dataset distillation. In *Proc. Adv. Neural Inform. Process. Syst.*, 2024b.
- Sandler, M., Howard, A., Zhu, M., Zhmoginov, A., and Chen, L.-C. Mobilenetv2: Inverted residuals and linear bottlenecks. In *Proc. IEEE Conf. Comput. Vis. Pattern Recog.*, pp. 4510–4520, 2018.
- Settles, B. Active learning literature survey. 2009.
- Shannon, C. E. A mathematical theory of communication. *The Bell system technical journal*, 27(3):379–423, 1948.
- Shao, S., Yin, Z., Zhou, M., Zhang, X., and Shen, Z. Generalized large-scale data condensation via various backbone and statistical matching. In *Proc. IEEE Conf. Comput. Vis. Pattern Recog.*, 2024a.
- Shao, S., Zhou, Z., Chen, H., and Shen, Z. Elucidating the design space of dataset condensation. *arXiv preprint arXiv:2404.13733*, 2024b.
- Shen, Z., Sherif, A., Yin, Z., and Shao, S. Delt: A simple diversity-driven early/late training for dataset distillation, 2024.
- Shin, S., Bae, H., Shin, D., Joo, W., and Moon, I.-C. Loss-curvature matching for dataset selection and condensation. In *International Conference on Artificial Intelligence and Statistics*, pp. 8606–8628, 2023.
- Sorscher, B., Geirhos, R., Shekhar, S., Ganguli, S., and Morcos, A. Beyond neural scaling laws: beating power law scaling via data pruning. In *Proc. Adv. Neural Inform. Process. Syst.*, pp. 19523–19536, 2022.
- Su, D., Hou, J., Gao, W., Tian, Y., and Tang, B. D⁴m: Dataset distillation via disentangled diffusion model. In *Proc. IEEE Conf. Comput. Vis. Pattern Recog.*, pp. 5809–5818, June 2024.
- Sun, P., Shi, B., Yu, D., and Lin, T. On the diversity and realism of distilled dataset: An efficient dataset distillation paradigm. In *Proc. IEEE Conf. Comput. Vis. Pattern Recog.*, 2024.
- Tan, M. and Le, Q. Efficientnet: Rethinking model scaling for convolutional neural networks. In *Proc. Int. Conf. Mach. Learn.*, pp. 6105–6114. PMLR, 2019.
- Toneva, M., Sordani, A., des Combes, R. T., Trischler, A., Bengio, Y., and Gordon, G. J. An empirical study of example forgetting during deep neural network learning. In *Proc. Int. Conf. Learn. Represent.*, 2019.
- Vicol, P., Lorraine, J. P., Pedregosa, F., Duvenaud, D., and Grosse, R. B. On implicit bias in overparameterized bilevel optimization. In *Proc. Int. Conf. Mach. Learn.*, pp. 22234–22259, 2022.

- Wang, K., Zhao, B., Peng, X., Zhu, Z., Yang, S., Wang, S., Huang, G., Bilen, H., Wang, X., and You, Y. Cafe: Learning to condense dataset by aligning features. In *Proc. IEEE Conf. Comput. Vis. Pattern Recog.*, pp. 12196–12205, 2022.
- Wang, K., Gu, J., Zhou, D., Zhu, Z., Jiang, W., and You, Y. Dim: Distilling dataset into generative model. *arXiv preprint arXiv:2303.04707*, 2023.
- Wang, T., Zhu, J.-Y., Torralba, A., and Efros, A. A. Dataset distillation. *arXiv preprint arXiv:1811.10959*, 2018.
- Xia, X., Liu, J., Yu, J., Shen, X., Han, B., and Liu, T. Moderate coreset: A universal method of data selection for real-world data-efficient deep learning. In *Proc. Int. Conf. Learn. Represent.*, 2023.
- Xiao, L. and He, Y. Are large-scale soft labels necessary for large-scale dataset distillation? In *Proc. Adv. Neural Inform. Process. Syst.*, 2024.
- Xu, A. and Raginsky, M. Information-theoretic analysis of generalization capability of learning algorithms. *Advances in neural information processing systems*, 30, 2017.
- Xu, Y., Li, Y.-L., Cui, K., Wang, Z., Lu, C., Tai, Y.-W., and Tang, C.-K. Distill gold from massive ores: Bi-level data pruning towards efficient dataset distillation. In *Proc. Eur. Conf. Comput. Vis.*, pp. 240–257. Springer, 2025.
- Yin, Z. and Shen, Z. Dataset distillation via curriculum data synthesis in large data era. *Transactions on Machine Learning Research*, 2024.
- Yin, Z., Xing, E., and Shen, Z. Squeeze, recover and relabel: Dataset condensation at imagenet scale from a new perspective. In *Proc. Adv. Neural Inform. Process. Syst.*, 2023.
- Yu, R., Liu, S., and Wang, X. Dataset distillation: A comprehensive review. *IEEE Transactions on Pattern Analysis and Machine Intelligence*, 2023.
- Yu, R., Liu, S., Ye, J., and Wang, X. Teddy: Efficient large-scale dataset distillation via taylor-approximated matching. In *Proc. Eur. Conf. Comput. Vis.*, pp. 1–17. Springer, 2025.
- Yun, S., Han, D., Oh, S. J., Chun, S., Choe, J., and Yoo, Y. Cutmix: Regularization strategy to train strong classifiers with localizable features. In *Proc. Int. Conf. Comput. Vis.*, pp. 6023–6032, 2019.
- Zhang, H. mixup: Beyond empirical risk minimization. *arXiv preprint arXiv:1710.09412*, 2017.
- Zhang, L., Zhang, J., Lei, B., Mukherjee, S., Pan, X., Zhao, B., Ding, C., Li, Y., and Xu, D. Accelerating dataset distillation via model augmentation. In *Proc. IEEE Conf. Comput. Vis. Pattern Recog.*, 2023.
- Zhang, X., Du, J., Li, Y., Xie, W., and Zhou, J. T. Spanning training progress: Temporal dual-depth scoring (tdds) for enhanced dataset pruning. In *Proceedings of the IEEE/CVF Conference on Computer Vision and Pattern Recognition*, pp. 26223–26232, 2024a.
- Zhang, X., Du, J., Liu, P., and Zhou, J. T. Breaking class barriers: Efficient dataset distillation via inter-class feature compensator. *arXiv preprint arXiv:2408.06927*, 2024b.
- Zhao, B. and Bilen, H. Dataset condensation with differentiable siamese augmentation. In *Proc. Int. Conf. Mach. Learn.*, pp. 12674–12685, 2021.
- Zhao, B. and Bilen, H. Synthesizing informative training samples with GAN. In *NeurIPS 2022 Workshop on Synthetic Data for Empowering ML Research*, 2022.
- Zhao, B. and Bilen, H. Dataset condensation with distribution matching. In *Proc. IEEE Winter Conf. Appl. Comput. Vis.*, pp. 6514–6523, 2023.
- Zhao, B., Mopuri, K. R., and Bilen, H. Dataset condensation with gradient matching. In *Proc. Int. Conf. Learn. Represent.*, 2021.
- Zheng, H., Liu, R., Lai, F., and Prakash, A. Coverage-centric coreset selection for high pruning rates. In *Proc. Int. Conf. Learn. Represent.*, 2023.
- Zhou, Y., Nezhadarya, E., and Ba, J. Dataset distillation using neural feature regression. In *Proc. Adv. Neural Inform. Process. Syst.*, 2022.

Appendix

A. Proof

A.1. Definitions

Definition A.1 (Negative Log-Likelihood (NLL)). Consider a dataset $\mathcal{D} = \{(x_i, y_i)\}_{i=1}^N$ and a model $p_\theta(y | x)$ parameterized by θ . The *Negative Log-Likelihood* is defined as the average negative log-probability of the observed data:

$$\text{NLL}(\mathcal{D}; \theta) = -\frac{1}{N} \sum_{i=1}^N \log p_\theta(y_i | x_i).$$

Remark A.2. The Negative Log-Likelihood can be interpreted as the empirical *Cross-Entropy* between the empirical distribution p (from \mathcal{D}) and the model distribution q_θ (from p_θ):

$$\text{NLL}(\mathcal{D}; \theta) \approx \text{CE}(p, q_\theta) = H(p) + D_{\text{KL}}(p \| q_\theta),$$

where $\text{CE}(p, q_\theta) = -\sum_x p(x) \log q_\theta(x)$ is the cross-entropy, $H(p)$ is the entropy of p , and D_{KL} is the Kullback–Leibler divergence. Minimizing NLL pushes q_θ closer to p .

Definition A.3 (Entropy (Shannon, 1948)). Entropy is an information-theoretic measure that quantifies the uncertainty or impurity in a probability distribution. For a classification problem with C classes, the entropy of a predictive distribution $p_\theta(y | x)$ is defined as (Settles, 2009):

$$H(Y | x; \theta) = -\sum_{y=1}^C p_\theta(y | x) \log p_\theta(y | x),$$

where $p_\theta(y | x)$ is the predicted probability of class y for input x , parameterized by θ . This measure captures the model’s uncertainty over the predicted classes for x .

A.2. Proof of Proposition 4.1

Assumption A.4 (Existence of a NLL-Reducing Crop). Let $\mathcal{C}_1, \mathcal{C}_2, \dots, \mathcal{C}_N$ be a set of N random crops for each sample (x_i, y_i) in the dataset $\mathcal{D} = \{(x_i, y_i)\}_{i=1}^N$. For each sample, there exists at least one index $k \in \{1, 2, \dots, N\}$ such that applying crop $\mathcal{C}_k(x_i)$ reduces the Negative Log-Likelihood (NLL) of the model:

$$\log p_\theta(y_i | \mathcal{C}_k(x_i)) < \log p_\theta(y_i | x_i).$$

Evidence. To validate the assumption, we calculate the Negative Log-Likelihood (NLL) for each random crop and compare it to the original NLL of the image using a pretrained model θ . We find that if the average probability of an increase in NLL is less than one, this indicates that at least once among the N random crops, the NLL decreases compared to the original image. As shown in Table 13, we can clearly see that the probability is less than 1.0 across various types of datasets.

Table 13: Average probability of increase in NLL. Standard deviation is computed from 100 random crops per image ($N = 100$) over the IPC10 dataset. The metric for determining the difficulty of the dataset is EL2N (Paul et al., 2021).

Crop Range = (r , 1.0)	Random	Hard + Balanced	Easy + Balanced
$r = 0.08$	0.72 ± 0.24	0.65 ± 0.27	0.63 ± 0.27
$r = 0.2$	0.68 ± 0.27	0.62 ± 0.29	0.60 ± 0.29
$r = 0.5$	0.63 ± 0.30	0.57 ± 0.32	0.59 ± 0.31
$r = 0.8$	0.59 ± 0.29	0.54 ± 0.31	0.59 ± 0.30

Lemma A.5 (Effect of Selective Cropping on NLL). *Under Assumption A.4, a selective cropping approach that chooses, for each sample, the crop minimizing its NLL can lower the average NLL of the dataset:*

$$\mathcal{L}(\mathcal{D}'; \theta) = \frac{1}{N} \sum_{i=1}^N \log p_{\theta}(y_i | \mathcal{C}_k(x_i)) < \mathcal{L}(\mathcal{D}; \theta),$$

where \mathcal{D}' is the selectively cropped dataset and $\mathcal{L}(\mathcal{D}; \theta)$ is the original dataset's average NLL.

Proof. Let $\mathcal{D} = \{(x_i, y_i)\}_{i=1}^N$ be the original dataset, and for each x_i , generate m crops $\mathcal{C}_j(x_i)$. Define

$$\mathcal{C}_{\min}(x_i) = \arg \min_{j \in \{1, \dots, m\}} \left[-\log p_{\theta}(y_i | \mathcal{C}_j(x_i)) \right].$$

Form the selective-crop dataset:

$$\mathcal{D}_{\text{select}} = \left\{ (\mathcal{C}_{\min}(x_i), y_i) : i = 1, \dots, N \right\}.$$

By construction,

$$-\log p_{\theta}(y_i | \mathcal{C}_{\min}(x_i)) \leq -\log p_{\theta}(y_i | x_i) \quad \forall i.$$

Hence, summing over i and dividing by N implies

$$\mathcal{L}(\mathcal{D}'; \theta) \leq \mathcal{L}(\mathcal{D}; \theta),$$

showing the overall NLL of \mathcal{D}' is no greater than that of the original dataset. □

Lemma A.6 (Correlation of NLL & Entropy). *Under a random cropping transformation $\mathcal{C} : \mathcal{X} \rightarrow \mathcal{X}$, the correlation between changes in average negative log-likelihood (NLL) $\mathcal{L}(\mathcal{D}; \theta)$ and changes in entropy $H(\mathcal{D}; \theta)$ is given by:*

$$\rho(\Delta\mathcal{L}, \Delta H) = \frac{\mathbb{E}[(\Delta\mathcal{L} - \mu_{\Delta\mathcal{L}})(\Delta H - \mu_{\Delta H})]}{\sigma_{\Delta\mathcal{L}}\sigma_{\Delta H}},$$

where $\Delta\mathcal{L}$ and ΔH represent changes in NLL and entropy, respectively. μ and σ are the corresponding means and standard deviations. The behavior of $\rho(\Delta\mathcal{L}, \Delta H)$ depends on dataset difficulty:

$$\rho(\Delta\mathcal{L}, \Delta H) = \begin{cases} < 0, & \text{if the dataset is easy or hard,} \\ > 0, & \text{if the dataset is moderate.} \end{cases}$$

For easy and hard datasets, cropping generally reduces NLL while increasing entropy. For moderate datasets, cropping increases NLL and reduces entropy, leading to a positive correlation.

Proof. Let $\mathcal{D} = \{(x_i, y_i)\}_{i=1}^N$ be a dataset, and let $\mathcal{C} : \mathcal{X} \rightarrow \mathcal{X}$ be a random cropping transformation. For each sample (x_i, y_i) , define the changes in NLL and entropy:

$$\Delta\mathcal{L}_i = \mathcal{L}(\mathcal{C}(x_i), y_i; \theta) - \mathcal{L}(x_i, y_i; \theta), \quad \Delta H_i = H(\mathcal{C}(x_i)) - H(x_i).$$

Here, \mathcal{L} is the negative log-likelihood under parameters θ , and $H(\cdot)$ is the Shannon entropy of the input.

Easy Datasets. These have prominent, localized features and redundant backgrounds. Random cropping typically removes non-informative regions, *reducing* \mathcal{L} (model becomes more confident) while *increasing* H (cropping induces greater image variability). Hence $\Delta\mathcal{L}_i < 0$ and $\Delta H_i > 0$. They move in opposite directions, so their covariance is negative, yielding $\rho(\Delta\mathcal{L}, \Delta H) < 0$.

Moderate Datasets. Contextual cues are crucial, so cropping removes essential information. This *increases* \mathcal{L} (model is less certain) and also *increases* H (more variability after losing context). Thus $\Delta\mathcal{L}_i > 0$ and $\Delta H_i > 0$. They move in the same direction, giving a positive covariance and $\rho(\Delta\mathcal{L}, \Delta H) > 0$.

Hard Datasets. Key features are subtle; cropping may sometimes remove distractors, slightly *decreasing* \mathcal{L} , while still *increasing* H . Thus $\Delta\mathcal{L}_i \lesssim 0$ and $\Delta H_i > 0$. Again, they vary inversely, so the covariance (and hence correlation) is negative.

Empirical Confirmation. Table 14 shows numerical evidence consistent with these three scenarios. Easy and hard datasets exhibit negative correlation between $\Delta\mathcal{L}$ and ΔH , while moderate datasets yield positive correlation.

Therefore, for random cropping in easy and hard datasets, $\Delta\mathcal{L}$ and ΔH typically move in opposite directions ($\rho < 0$), whereas in moderate datasets, they move in the same direction ($\rho > 0$), confirming the stated lemma.

Table 14: Correlation between Changes in NLL and Shannon Entropy under Various Dataset Conditions

Metric: EL2N (Paul et al., 2021)	Easy Only	Easy + Balanced	Random	Hard + Balanced	Hard Only
Correlation $\rho(\Delta\mathcal{L}, \Delta H)$	-0.70	0.66	0.46	0.03	-0.60
Concordant Direction Changes	0.25	0.87	0.85	0.56	0.29
$\Delta\mathcal{L}$ (mean \pm std)	-0.05 ± 0.48	0.21 ± 0.24	0.76 ± 0.74	0.66 ± 0.89	-0.10 ± 0.70
ΔH (mean \pm std)	0.21 ± 0.39	0.30 ± 0.48	0.62 ± 0.72	0.26 ± 0.69	0.23 ± 0.62

□

Proof of Proposition 4.1. Let $\mathcal{D}' = \mathcal{C}(\mathcal{D})$ denote the dataset transformed by selective cropping operation \mathcal{C} . We demonstrate the non-implication through three connected arguments: guaranteed NLL reduction, entropy behavior analysis, and explicit counterconstruction.

First, Lemma A.5 establishes that for any \mathcal{D} satisfying Assumption A.4, the selective cropping operation \mathcal{C} necessarily reduces the average negative log-likelihood:

$$\mathcal{L}(\mathcal{D}'; \theta) = \frac{1}{N} \sum_{i=1}^N -\log p_{\theta}(y_i | \mathcal{C}(x_i)) < \frac{1}{N} \sum_{i=1}^N -\log p_{\theta}(y_i | x_i) = \mathcal{L}(\mathcal{D}; \theta).$$

This follows directly from the selection mechanism $\mathcal{C}_{\min}(x_i) = \arg \min_j [-\log p_{\theta}(y_i | \mathcal{C}_j(x_i))]$, which ensures component-wise improvement.

Next consider the Shannon entropy $H(\mathcal{D}) = -\mathbb{E}_{x \sim \mathcal{D}}[\log p(x)]$. Lemma A.6 reveals the conditional relationship between NLL reduction and entropy changes:

$$\rho(\Delta\mathcal{L}, \Delta H) = \begin{cases} < 0, & \text{easy/hard datasets} \\ > 0, & \text{moderate datasets} \end{cases}$$

where $\Delta\mathcal{L} = \mathcal{L}(\mathcal{D}'; \theta) - \mathcal{L}(\mathcal{D}; \theta)$ and $\Delta H = H(\mathcal{D}') - H(\mathcal{D})$. For hard-only datasets (Table 14, last column), we observe:

$$\begin{aligned} \mathbb{E}[\Delta\mathcal{L}] &= -0.10 \pm 0.70 \\ \mathbb{E}[\Delta H] &= 0.23 \pm 0.62, \end{aligned}$$

demonstrating that NLL reduction ($\Delta\mathcal{L} < 0$) can coexist with entropy increase ($\Delta H > 0$).

This leads to our crucial counterexample: let $\mathcal{D}_{\text{hard}}$ be a dataset with $\rho(\Delta\mathcal{L}, \Delta H) = -0.60$. For this dataset:

$$\begin{aligned} \text{NLL}(\mathcal{D}'; \theta) &< \text{NLL}(\mathcal{D}; \theta) \quad (\text{by Lemma A.5}) \\ H(\mathcal{D}') &= H(\mathcal{D}) + \Delta H > H(\mathcal{D}) \quad (\text{from } \mathbb{E}[\Delta H] > 0). \end{aligned}$$

The simultaneous NLL reduction and entropy increase in $\mathcal{D}_{\text{hard}}$ provides an explicit counterexample to the universal claim that $\text{NLL}(\mathcal{D}') < \text{NLL}(\mathcal{D})$ implies $H(\mathcal{D}') < H(\mathcal{D})$.

The existence of such counterexamples stems from the fundamental difference between NLL and entropy: while NLL measures model confidence through $p_{\theta}(y|x)$, entropy quantifies input diversity via $p(x)$. Selective cropping optimizes for the

former while potentially increasing the latter, particularly in datasets where discriminative features are locally concentrated but globally varied across samples.

Thus, the proposition holds because we have identified concrete conditions (easy/hard datasets with EL2N extremes) where NLL reduction through cropping demonstrably fails to produce entropy reduction. \square

A.3. Proof for Theorem 4.2

Assumption A.7 (Entropy Increment of Cropping). Let \mathcal{X} be an input space and $\mathcal{C}_r : \mathcal{X} \rightarrow \mathcal{X}$ be a random cropping operation with crop ratio $r \in (0, 1]$. For any dataset $\mathcal{D} \subset \mathcal{X} \times \mathcal{Y}$, the following cases describe the expected entropy behavior:

Case 1. For a single cropping operation, the expected entropy of the cropped dataset exceeds the entropy of the original dataset:

$$\mathbb{E}[H(\mathcal{C}_r(\mathcal{D}))] > H(\mathcal{D}).$$

Case 2. When comparing two crop ratios $r_1, r_2 \in (0, 1]$ such that $r_1 < r_2$, the smaller ratio produces a larger expected entropy increment relative to the original dataset:

$$\mathbb{E}[H(\mathcal{C}_{r_1}(\mathcal{D}))] - H(\mathcal{D}) > \mathbb{E}[H(\mathcal{C}_{r_2}(\mathcal{D}))] - H(\mathcal{D}).$$

Case 3. For two consecutive cropping operations with ratios $r_1, r_2 \in (0, 1]$ such that $r_1 \cdot r_2 = r$, the expected entropy increment of the repeated cropping operation exceeds that of a single cropping operation with ratio r :

$$\mathbb{E}[H(\mathcal{C}_{r_2}(\mathcal{C}_{r_1}(\mathcal{D})))] - H(\mathcal{D}) > \mathbb{E}[H(\mathcal{C}_r(\mathcal{D}))] - H(\mathcal{D}).$$

Empirical Confirmation for Case 1. From Table 15, we can observe that regardless of different dataset difficulty, the expected entropy increases ($p > 0.5$).

Table 15: Average probability (p) of increase in entropy. Standard deviation is computed from 100 random crops per image ($N = 100$). The metric for determining the difficulty of the dataset is EL2N (Paul et al., 2021).

Crop Range	Easy Only	Easy + Balanced	Random	Hard + Balanced	Hard Only
$r = 0.08$	0.59 ± 0.28	0.60 ± 0.28	0.67 ± 0.26	0.58 ± 0.28	0.57 ± 0.28
$r = 0.2$	0.59 ± 0.29	0.58 ± 0.29	0.64 ± 0.28	0.56 ± 0.29	0.55 ± 0.29
$r = 0.5$	0.60 ± 0.31	0.57 ± 0.31	0.60 ± 0.30	0.55 ± 0.31	0.55 ± 0.31
$r = 0.8$	0.61 ± 0.30	0.58 ± 0.30	0.58 ± 0.29	0.55 ± 0.30	0.56 ± 0.30

Reasoning for Case 2. Smaller crop ratios (r_1) retain less of the original image, leading to a greater reduction in structural information and a more pronounced increase in randomness. For instance, a smaller crop of an image is less likely to preserve identifiable or contextually meaningful features. This introduces higher variability across the cropped dataset, leading to a larger entropy increment. In contrast, larger crop ratios (r_2) retain more of the original structure, limiting the entropy gain. Table 16 clearly indicates that entropy increases regardless of dataset difficulty as r decreases.

Reasoning for Case 3. Repeated cropping applies a second layer of randomness to the already cropped dataset. The first crop, $\mathcal{C}_{r_1}(\mathcal{D})$, introduces variability by sampling a subset of the original image. The second crop, \mathcal{C}_{r_2} , conditions its randomness on the already reduced structure of $\mathcal{C}_{r_1}(\mathcal{D})$, amplifying the total variability. This compounding randomness makes the expected entropy increment greater than that of a single crop $\mathcal{C}_r(\mathcal{D})$ with the same total ratio r . Evidence of the claim is supported by Table 16, where the entropy increment of two repeated crops is consistently greater than a single crop despite having the same final cropping ratio.

Table 16: Average entropy change across different crop ranges. Values are computed from 100 random crops per image ($N = 100$). Value 1 (Value 2) denotes the entropy increment from a single crop r or **two repeated crops** $r^{\frac{1}{2}}$, where $r < 0$. The metric for determining the difficulty of the dataset is EL2N (Paul et al., 2021).

Crop Range	Easy Only	Easy + Balanced	Random	Hard + Balanced	Hard Only
$r = 0.08$	0.21 (0.22)	0.30 (0.35)	0.63 (0.84)	0.26 (0.32)	0.23 (0.27)
$r = 0.2$	0.12 (0.15)	0.15 (0.19)	0.44 (0.55)	0.16 (0.21)	0.13 (0.17)
$r = 0.5$	0.09 (0.13)	0.08 (0.12)	0.21 (0.28)	0.10 (0.15)	0.09 (0.12)
$r = 0.8$	0.07 (0.10)	0.06 (0.09)	0.10 (0.14)	0.07 (0.10)	0.06 (0.09)

Lemma A.8 (Uncertainty and Generalization). *In small-data regimes, lower predictive uncertainty (i.e., smaller entropy $H(Y | x; \theta)$) correlates with better generalization performance.*

Proof. Let $\mathcal{D} = \{(x_i, y_i)\}_{i=1}^N$ be drawn i.i.d. from a distribution μ on $\mathcal{X} \times \mathcal{Y}$. Suppose a (possibly stochastic) learning algorithm \mathcal{M} , when given \mathcal{D} , produces parameters $\theta = \mathcal{M}(\mathcal{D}) \in \Theta$. Denote by $p_\theta(y | x)$ the model’s predictive distribution and by the predictive entropy for an input x :

$$H(Y | x; \theta) = - \sum_{c=1}^C p_\theta(c | x) \log p_\theta(c | x).$$

A lower value of this entropy indicates that the model is more confident in its prediction for x , and entropy is a general measure of uncertainty (Settles, 2009; Coleman et al., 2020).

Information-theoretical analysis on generalization (Xu & Raginsky, 2017) shows that if θ depends on \mathcal{D} , then

$$\mathbb{E}[L_\mu(\theta) - L_{\mathcal{D}}(\theta)] \leq \sqrt{\frac{2 \sigma^2 I(\mathcal{D}; \theta)}{N}},$$

where $L_\mu(\theta)$ is the population risk, $L_{\mathcal{D}}(\theta)$ is the empirical risk on \mathcal{D} , σ^2 is an upper bound on the loss variance, and $I(\mathcal{D}; \theta)$ is the mutual information between \mathcal{D} and θ . A smaller $I(\mathcal{D}; \theta)$ tightens this bound, leading to a smaller gap between training and test performance. In small-data settings, σ^2 can be comparatively large because each sample exerts a bigger influence on the loss, so keeping $I(\mathcal{D}; \theta)$ low is especially important for controlling the generalization error.

Thus, lower predictive entropy (i.e., lower uncertainty) typically corresponds to lower $I(\mathcal{D}; \theta)$, yielding a tighter generalization bound. Because a small N often makes σ^2 relatively more influential in the bound, this effect is pronounced in small-data regimes, and models that maintain lower predictive uncertainty across \mathcal{D} tend to achieve better generalization performance. Similar findings that keep lower uncertainty data are also found in (Sorscher et al., 2022; He et al., 2024). \square

Proof of Theorem 4.2. Let \mathcal{D} be a dataset with entropy $H(\mathcal{D})$, and let $\mathcal{D}' = \mathcal{C}_{r_1}(\mathcal{D})$ be a selectively cropped version such that $H(\mathcal{D}') < H(\mathcal{D})$, where \mathcal{C}_{r_1} represents a cropping operation with ratio $r_1 \in (0, 1)$. Consider an augmentation strategy \mathcal{A} that includes random cropping operations with ratio $r_2 \in (0, 1)$, and let p_θ be a model pretrained on \mathcal{D} using \mathcal{A} .

When we apply the augmentation \mathcal{A} to \mathcal{D} and \mathcal{D}' , the expected entropies of the augmented datasets are:

$$\begin{aligned} \mathbb{E}[H(\mathcal{A}(\mathcal{D}))] &= H(\mathcal{D}) + \Delta H, \\ \mathbb{E}[H(\mathcal{A}(\mathcal{D}'))] &= H(\mathcal{D}') + \Delta H', \end{aligned}$$

where ΔH and $\Delta H'$ denote the expected entropy increments due to the augmentation \mathcal{A} applied to \mathcal{D} and \mathcal{D}' , respectively.

From **Assumption A.7** (Case 3), applying a random crop to the already cropped dataset \mathcal{D}' is equivalent to applying two consecutive cropping operations to \mathcal{D} : first with ratio r_1 (the selective crop) and then with ratio r_2 (the random crop in \mathcal{A}). The combined effective crop ratio is $r = r_1 \cdot r_2$.

According to Case 3, the expected entropy increment from two consecutive crops exceeds that of a single crop with the same total crop ratio:

$$\Delta H' = \mathbb{E}[H(\mathcal{C}_{r_2}(\mathcal{C}_{r_1}(\mathcal{D}))) - H(\mathcal{D})] > \mathbb{E}[H(\mathcal{C}_r(\mathcal{D})) - H(\mathcal{D})] = \Delta H.$$

This implies that:

$$\Delta H' > \Delta H.$$

Now, consider the difference in expected entropy after augmentation:

$$\begin{aligned} \mathbb{E}[H(\mathcal{A}(\mathcal{D}'))] - \mathbb{E}[H(\mathcal{A}(\mathcal{D}))] &= (H(\mathcal{D}') + \Delta H') - (H(\mathcal{D}) + \Delta H) \\ &= (H(\mathcal{D}') - H(\mathcal{D})) + (\Delta H' - \Delta H). \end{aligned}$$

Since $H(\mathcal{D}') < H(\mathcal{D})$, let $\delta H = H(\mathcal{D}) - H(\mathcal{D}') > 0$. Then:

$$\mathbb{E}[H(\mathcal{A}(\mathcal{D}'))] - \mathbb{E}[H(\mathcal{A}(\mathcal{D}))] = -\delta H + (\Delta H' - \Delta H).$$

For the difference in entropy after augmentation to be positive, we require:

$$\Delta H' - \Delta H > \delta H.$$

This means that the increase in the entropy increment due to applying \mathcal{A} to \mathcal{D}' must exceed the initial entropy reduction δH caused by the selective cropping.

From the empirical observations in Table 16, we see that the entropy increment from two consecutive crops (shown as Value 2) is consistently greater than that from a single crop (shown as Value 1), and the difference between $\Delta H'$ and ΔH increases with smaller crop ratios. Specifically, the entropy increments satisfy:

$$\Delta H' \approx \Delta H + \epsilon,$$

where $\epsilon > \delta H$, based on the empirical data indicating that the compounded increase in entropy surpasses the initial reduction.

Therefore, we have:

$$-\delta H + (\Delta H' - \Delta H) > 0 \implies \mathbb{E}[H(\mathcal{A}(\mathcal{D}'))] > \mathbb{E}[H(\mathcal{A}(\mathcal{D}))].$$

This means that the expected entropy after augmentation is higher for \mathcal{D}' :

$$H_{p_\theta}(\mathcal{A}(\mathcal{D}')) > H_{p_\theta}(\mathcal{A}(\mathcal{D})).$$

According to **Lemma A.8**, in small-data regimes, higher predictive uncertainty (i.e., higher entropy) correlates with worse generalization performance. Therefore, the model's performance metric satisfies:

$$\mathcal{P}(\mathcal{A}(\mathcal{D}')) < \mathcal{P}(\mathcal{A}(\mathcal{D})).$$

Thus, under the given conditions, the entropy evaluated by the model on $\mathcal{A}(\mathcal{D}')$ does not directly reflect the image quality of \mathcal{D}' , and the model's performance on $\mathcal{A}(\mathcal{D}')$ is worse than on $\mathcal{A}(\mathcal{D})$.

□

B. Experiment Settings

B.1. Dataset and Network

Dataset. The ImageNet-1K dataset (Deng et al., 2009), also known as ILSVRC-2012, is a large-scale image classification dataset containing $N = 1.28$ million training images and 50,000 validation images across $K = 1,000$ object categories. Each image is manually annotated with a single class label. The dataset contains approximately 1,200 images per class in the training set. Images have an average resolution of 469×387 pixels but are typically pre-processed to a standard size of 224×224 pixels for model training. This dataset has become a de facto benchmark for evaluating deep learning models in computer vision tasks, particularly for image classification problems.

Network. For all networks, we use common network definition from <https://pytorch.org/vision/main/models.html>. Networks are trained for 300 epochs by default; detailed settings are provided in Appendix B.2.

B.2. Standard Evaluation Setting

Table 17 provides a more comprehensive comparison among baseline dataset distillation methods. We have adopted the CDA’s setting (Yin & Shen, 2024) as the **standard evaluation setting** for two main reasons: (1) many other studies, such as LPLD (Xiao & He, 2024) and DWA (Du et al., 2024), have used this setting; and (2) it applies to most methods, being designed explicitly for datasets that include combined image patterns, in contrast to patch shuffling. Note that baseline dataset pruning methods also adhere to the **standard evaluation setting** for fair comparison.

It’s important to note that using alternative settings or additional techniques is **NOT** incorrect; however, we have chosen a standard evaluation setting to facilitate a clearer comparison among the different methods.

Table 17: Inconsistent evaluation settings of Dataset Distillation on ImageNet-1K. Values marked in red are settings different from SRe²L. † represents the IPC-dependent.

Configuration	Value	SRe ² L (Yin et al., 2023)	CDA (Yin & Shen, 2024)	LPLD (Xiao & He, 2024)	DWA (Du et al., 2024)	RDED (Sun et al., 2024)	G-VBSM (Shao et al., 2024a)	EDC (Shao et al., 2024b)
Epochs	300	✓	✓	✓	✓	✓	✓	✓
Optimizer	AdamW	✓	✓	✓	✓	✓	✓	✓
Model LR	0.001	✓	✓	✓	✓	✓	✓	✓
LR	Smooth LR	✗	✗	✗	✗	✓	✗	✓
LR Scheduler	CosineAnnealing	✓	✓	✓	✓	✓	✓	✓
Batch Size	1024	1024	128	128	128	100 [†]	1024	100
Soft Label	Single / Ensemble	Single	Single	Single	Single	Single	Ensemble	Ensemble
Loss Type	KL / MSE+0.1xGT	KL	KL	KL	KL	KL	MSE	MSE
EMA-based	✗	✗	✗	✗	✗	✗	✗	✓
	PatchShuffle	✗	✗	✗	✗	✓	✗	✓
	ResizedCrop	✓	✓	✓	✓	✓	✓	✓
Augmentation	CropRange	(0.08, 1)	(0.08, 1)	(0.08, 1)	(0.08, 1)	(0.5, 1)	(0.08, 1)	(0.5, 1)
	Flip	✓	✓	✓	✓	✓	✓	✓
	Cut-Mix	✓	✓	✓	✓	✓	✓	✓

Remark: Table 17 does not cover all the different settings. For example, EDC (Shao et al., 2024b) uses EMA-based evaluation while other methods do not include it.

B.3. Fair Storage of Pruning Datasets

When considering the pruning ratio in state-of-the-art (SOTA) pruning methods, it is important to note that the pruning ratio does not directly correspond to the dataset distillation setting. Existing pruning techniques primarily focus on tracking the ranking of images (i.e., the indices) rather than storing the actual dataset, which leads to the neglect of the true size of the ImageNet-1K images. Additionally, dataset distillation limits image resolution to 224×224 pixels. Therefore, it is unfair, in terms of information content and storage, to directly store the actual ImageNet-1K images, which have a higher average resolution of 469×387 pixels. To address this, we choose to crop the images based on their shortest side and then resize them to 224×224 pixels.

B.4. Baselines Specifications

In this section, we provide more specifications of each baseline.

Dataset Distillation Baselines:

- **SRe²L (Yin et al., 2023)**: No special adjustments. Dataset recovered following <https://github.com/VILA-Lab/SRe2L>.
- **CDA (Yin & Shen, 2024)**: No special adjustments; results reported are from the original paper. Dataset recovered following <https://github.com/VILA-Lab/CDA>.
- **G-VBSM (Shao et al., 2024a)**: No special adjustments. Dataset recovered following https://github.com/shaoshitong/G-VBSM_Dataset_Condensation.
- **LPLD (Xiao & He, 2024)**: No special adjustments; results reported are from the original paper. Dataset provided in <https://github.com/he-y/soft-label-pruning-for-dataset-distillation>.
- **DWA (Du et al., 2024)**: No special adjustments; results reported are from the original paper. Dataset recovered following <https://github.com/AngusDujw/Diversity-Driven-Synthesis>.
- **RDED (Sun et al., 2024)**: IPC10 and IPC50 selects patch from $m = 300$ patches, and IPC100 selects from $m = 600$ patches. Dataset recovered following <https://github.com/LINs-lab/RDED>.

Dataset Pruning Baselines: We create datasets by using the data ranking scores provided by Zheng et al. (<https://github.com/haizhongzheng/Coverage-centric-coreset-selection>). After obtaining the ranking, we post-process the datasets into images of resolution 224×224 , according to Appendix B.3.

- **Forgetting (Toneva et al., 2019)**: Images with low “forgetting events” are selected; if images have a same number of “forgetting events”, we randomly sample the images. Strict class balance is enforced.
- **EL2N (Paul et al., 2021)**: Images with low “EL2N Scores” are selected; and strict class balance is enforced.
- **AUM (Pleiss et al., 2020)**: Images with high “accumulated margin” are selected; strict class balance is enforced.
- **CCS (Zheng et al., 2023)**: For the base pruning metric, we use AUM (Pleiss et al., 2020) following the original experiment setting. In addition, we prune away 30% “misabeled” data for IPC10 and IPC50, and 20% “misabeled” data are removed for IPC100 due to strict class balance requiring enough images for each class.

C. Main Result with Standard Deviation

C.1. Soft Label Benchmarks with Standard Deviation

Table 18: Benchmarking SOTA methods against random baseline under evaluation with **soft labels**. † means optimization-free distillation. ResNet-18 on ImageNet-1K. Standard deviations are computed from three independent runs.

IPC	Random	DD with Noise Initialization				DD with Real Initialization		Pruning Method with Rules			
		SRe ² L	CDA	G-VBSM	LPLD	RDED [†]	DWA	Forgetting	EL2N	AUM	CCS
10	35.8±0.2	33.5±0.2	33.5±0.3	35.8±0.7	34.6±0.9	38.4±0.1	37.9±0.2	36.1±0.3	40.8±0.4	41.5±0.1	37.4±0.2
50	57.2±0.2	52.6±0.1	53.5±0.3	54.8±0.2	55.4±0.3	56.2±0.2	55.2±0.2	57.2±0.1	58.1±0.1	58.5±0.1	58.2±0.1
100	61.2±0.2	57.4±0.3	58.0±0.2	59.2±0.1	59.4±0.2	60.2±0.1	59.2±0.3	61.0±0.1	61.5±0.2	61.5±0.1	61.6±0.1

C.2. Hard Label Benchmarks with Standard Deviation

Table 19: Benchmarking SOTA methods against random baseline under evaluation with **hard labels**. † means optimization-free distillation. ResNet-18 on ImageNet-1K. Standard deviations are computed from three independent runs.

IPC	Random	DD with Noise Initialization				DD with Real Initialization		Pruning Method with Rules				PCA Framework
		SRe ² L	CDA	G-VBSM	LPLD	RDED [†]	DWA	Forgetting	EL2N	AUM	CCS	Ours [†]
10	4.6±0.1	1.5±0.1	1.6±0.1	1.6±0.1	3.4±0.1	11.5±0.1	1.9±0.0	3.4±0.1	12.2±0.3	11.4±0.0	6.8±0.3	22.8±0.3
50	20.6±0.1	3.8±0.0	5.8±0.3	9.0±0.6	5.1±0.1	30.8±0.4	5.3±0.2	11.7±0.2	31.1±0.3	30.6±0.1	29.3±0.4	39.1±0.2
100	31.7±0.6	4.9±0.2	8.0±0.1	16.6±0.6	6.0±0.1	39.2±0.6	7.5±0.1	18.3±0.2	38.7±0.1	38.8±0.2	39.0±0.4	45.5±0.4

D. Additional Experiments and Analysis

D.1. Training with Noisy Images

From Table 3, we can see that even with **purely noisy images**, the student network is able to learn from the teacher network by matching the soft labels. This is surprising, as noisy images are typically not expected to contain any useful information for the network’s learning process. Nevertheless, the performance of 0.5% is significant compared to the purely random network’s performance of 0.1%.

Table 20: Distillation training with pure noise on ResNet-18 on ImageNet-1K. ‘BS’ denotes batch size.

	Expected Acc.	BS=128	BS=1024
IPC50	0.1 %	0.5 %	0.3 %

D.2. Use Real Images as Initialization for Dataset Distillation

As shown in Figure 2, we categorize existing literature into three distinct sections. The first section encompasses dataset distillation with **noise** initialization, where no images from the original dataset are directly involved. The representative work in this category is SRe²L (Yin et al., 2023), which pioneered this approach. The second section comprises dataset distillation with **real** image initialization, where the number of original images directly involved equals the distilled dataset size (specifically, $IPC \times 1000$ images). An exception is RDED (Sun et al., 2024), which randomly samples m images and combines crops, utilizing $m \times 1000$ images, where $m > IPC$. The final section focuses on dataset pruning methods, which evaluate the entire dataset to identify optimal subsets, thereby involving all images directly in the dataset compression process.

To validate the significance of incorporating more original images, we reimplemented SRe²L with real images as initialization. Table 21 demonstrates that merely initializing with real images consistently improves performance across both soft-label and hard-label benchmarks.

Table 21: Performance of SRe²L with real images as initialization.

	Soft Label			Hard Label		
	Random	SRe ² L	SRe ² L _{Real}	Random	SRe ² L	SRe ² L _{Real}
10	35.8 \pm 0.2	33.5 \pm 0.2	35.3 \pm 0.5	4.6 \pm 0.1	1.5 \pm 0.1	2.5 \pm 0.0
50	57.2 \pm 0.2	52.6 \pm 0.1	53.9 \pm 0.3	20.6 \pm 0.1	3.8 \pm 0.0	6.3 \pm 0.2
100	61.2 \pm 0.2	57.4 \pm 0.3	58.3 \pm 0.1	31.7 \pm 0.6	4.9 \pm 0.2	7.9 \pm 0.2

D.3. Regularization-based Data Augmentation

Table 22 presents a comprehensive evaluation of various data augmentation strategies, including CutMix (Yun et al., 2019), Cutout (DeVries & Taylor, 2017), and Mixup (Zhang, 2017). The experimental results demonstrate the **crucial role of appropriate augmentation selection** in data-scarce scenarios. The incorporation of *RandomResizedCrop* proves to be fundamental, substantially improving performance from 21.6% to 25.6%.

Among the regularization-based augmentation techniques, Cutout demonstrates a better performance, maintaining consistent accuracy levels (26.2%, 25.7%, and 25.3% with *RandomResizedCrop*). This superiority can be attributed to two key factors: First, Cutout preserves label integrity by avoiding label mixing, which is particularly beneficial in data-scarce regimes. Second, its augmentations are performed on individual images without cross-sample interactions, adhering to the principle of maintaining sample simplicity during training. In contrast, both CutMix and Mixup show notable performance degradation with increased mixing probabilities, which is especially evident in scenarios with label mixing. When label mixing is employed, performance deteriorates significantly (from 25.5% to 23.8% for CutMix, and from 25.9% to 25.7% for Mixup at 0.2 mixing probability with *RandomResizedCrop*). This degradation becomes more severe at higher mixing probabilities, with performance dropping to 17.4% and 7.7%, respectively, at 1.0 mixing probability.

These findings align with our theoretical framework, suggesting that augmentation strategies maintaining sample simplicity are more effective in data-scarce regimes. The empirical evidence demonstrates that methods introducing complex regularization through label mixing and cross-sample interactions may be detrimental to model performance when training data is limited, supporting our scaling law observations regarding the preference for simpler training samples.

Setting for each strategy:

- CutMix (Yun et al., 2019): We follow the original implementation which samples from $\text{Beta}(\alpha, \alpha)$, where $\alpha = 1$, which is basically uniform sampling from $(0, 1)$. For the label mixing part, we rescale λ following <https://github.com/clovaai/CutMix-PyTorch>.
- Mixup (Zhang, 2017): We follow the original implementation which samples from $\text{Beta}(\alpha, \alpha)$, where $\alpha = 1$, which is basically uniform sampling from $(0, 1)$.
- Cutout (DeVries & Taylor, 2017): We use a common cutout size which is 0.5.

Remark: In the original implementation of SRe²L, CutMix and Mixup do not incorporate label mixing because distillation loss is used.

Table 22: Experiments with regularization-based data augmentation of PCA (Ours) in the SGD setting. For *RandomResizedCrop*, the default setting is used, which crop in the range of $(0.08, 1.00)$. The mix probability refers to the likelihood of performing data mixing, where a value of 1.0 indicates that data mixing is always conducted. When *RandomResizedCrop* is \times , it means to use regularization-based data augmentation to entirely replace *RandomResizedCrop*. Experiments are conducted on ResNet-18, IPC10 of ImageNet-1K.

Crop	Data Mixing	Label Mixing	Mix Probability			Crop	Data Mixing	Label Mixing	Mix Probability		
			0.2	0.5	1.0				0.2	0.5	1.0
✓	✗	-	25.6			✗	✗	-	21.6		
✓	CutMix	✓	23.8	23.0	17.4	✗	CutMix	✓	9.8	8.1	10.5
		✗	25.5	24.7	23.0			✗	15.6	14.3	12.5
✓	Mixup	✓	25.7	23.0	7.7	✗	Mixup	✓	18.9	17.4	8.4
		✗	25.9	25.1	17.6			✗	19.2	18.3	15.6
✓	Cutout	-	26.2	25.7	25.3	✗	Cutout	-	22.7	22.4	21.8

D.4. Poor Performance using Forgetting (Toneva et al., 2019)

Fig. 6 illustrates the distribution of various score metrics, specifically EL2N (Paul et al., 2021), Forgetting (Toneva et al., 2019), and AUM (Pleiss et al., 2020) Scores. These distributions are organized into two rows, with the top row representing the full dataset and the bottom row depicting the “easiest” IPC10 subset.

In the analysis of the **EL2N Score**, the histogram for the full dataset shows a unimodal distribution that peaks around a score of 10, indicating that most scores are concentrated in this range. Additionally, there is a long tail in the distribution towards lower scores.

Examining the **Forgetting Score**, the Full dataset displays a bimodal distribution with significant frequencies at scores of 0 and 10. This bimodality indicates the presence of two prevalent score categories within the complete dataset. Conversely, the IPC10 Forget Score distribution is dominated by a sharp peak at score 0, reflecting a substantial proportion of instances with no forgetting behavior in the IPC10 subset.

Regarding the **AUM Score**, the Full dataset illustrates a symmetric distribution centered around a score of 0, indicating balanced score dispersion. The IPC10 AUM Score distribution, however, shows a broader range with a prominent peak near 56 and a gradual decline as scores approach 60. This shift suggests that the IPC10 subset experiences a different range of AUM Scores compared to the full dataset.

The poor performance of forgetting can possibly be explained by the score distribution (see Fig. 6). We can clearly see that the easiest IPC10 subsets of forgetting scores all have a value of “0,” indicating that no forgetting occurs. Because of the nature of the forgetting approach, many images experience no forgetting events at all. In fact, there are approximately

110,000 images without any forgetting events, and we randomly selected 10,000 (roughly 9.1%) of these images to create our IPC10 dataset. As a result, the 10,000 images are **indistinguishable** from the remaining images (90.9%) that also have zero forgetting counts.

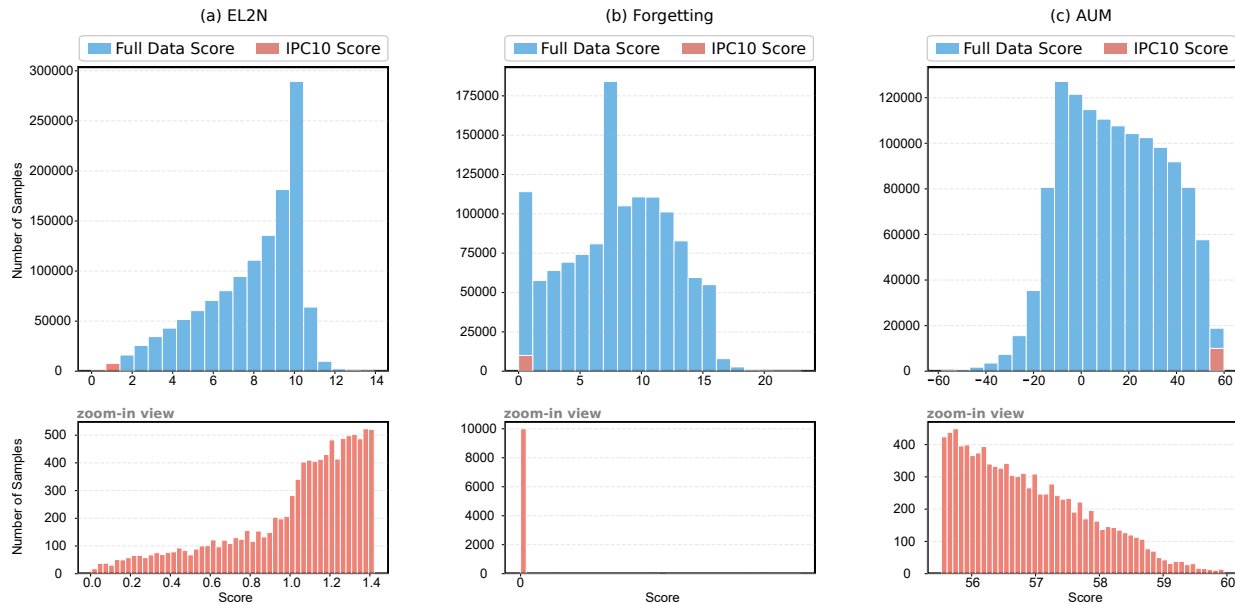


Figure 6: Sample distribution over the score of different pruning metrics: (a) EL2N, (b) Forgetting, and (c) AUM. Top row: both the sample distribution of full and IPC10 datasets. Bottom row: zoomed-in view of the distribution of IPC10 dataset. IPC10 datasets are selected from the “easiest” samples.

D.5. Strict Data Balance Is an Implicit Stratification

Figure 7 (Top) illustrates the distribution of samples across different classes. A clear severe class imbalance is observed when samples are selected solely based on pruning scores, as shown by the red histogram. Some classes have no images at all, while others contain more than 100 images. This imbalance is particularly noticeable when using Forgetting as the pruning metric.

By enforcing strict class balance, the difficulty of the subset increases as long as class imbalance persists. This is demonstrated in Figure 7 (Bottom), where higher scores in EL2N and Forgetting indicate a harder dataset, while a lower score in AUM suggests the opposite. Consequently, strict class balance implicitly achieves data stratification (Zheng et al., 2023) among easy samples, and it can partly explain Table 23 why adding additional explicit stratification does not improve the performance as suggested by CCS (Zheng et al., 2023). Additional stratification applied after strict balancing increases dataset complexity, with particularly noticeable effects in small IPC scenarios.

Table 23: CCS performance comparison on soft and hard label settings. CCS_{AUM} denotes stratification performed on AUM.

Setting	IPC	Random	Forgetting	AUM	EL2N	CCS_{AUM}
Soft	10	35.8 \pm 0.2	36.1 \uparrow 0.3	41.5 \uparrow 5.7	40.8 \uparrow 5.0	37.4 \uparrow 1.6
	50	57.2 \pm 0.2	57.2 \pm 0.0	58.5 \uparrow 1.3	58.1 \uparrow 0.9	58.2 \uparrow 1.0
	100	61.2 \pm 0.2	61.0 \downarrow 0.2	61.5 \uparrow 0.3	61.5 \uparrow 0.3	61.6 \uparrow 0.4
Hard	10	4.6 \pm 0.1	3.4 \downarrow 1.2	11.4 \uparrow 6.8	12.2 \uparrow 7.6	6.8 \uparrow 2.2
	50	20.6 \pm 0.1	11.7 \downarrow 8.9	30.6 \uparrow 10.0	31.1 \uparrow 10.5	29.3 \uparrow 8.7
	100	31.7 \pm 0.6	18.3 \downarrow 13.4	38.7 \uparrow 7.0	38.8 \uparrow 7.1	39.0 \uparrow 7.3

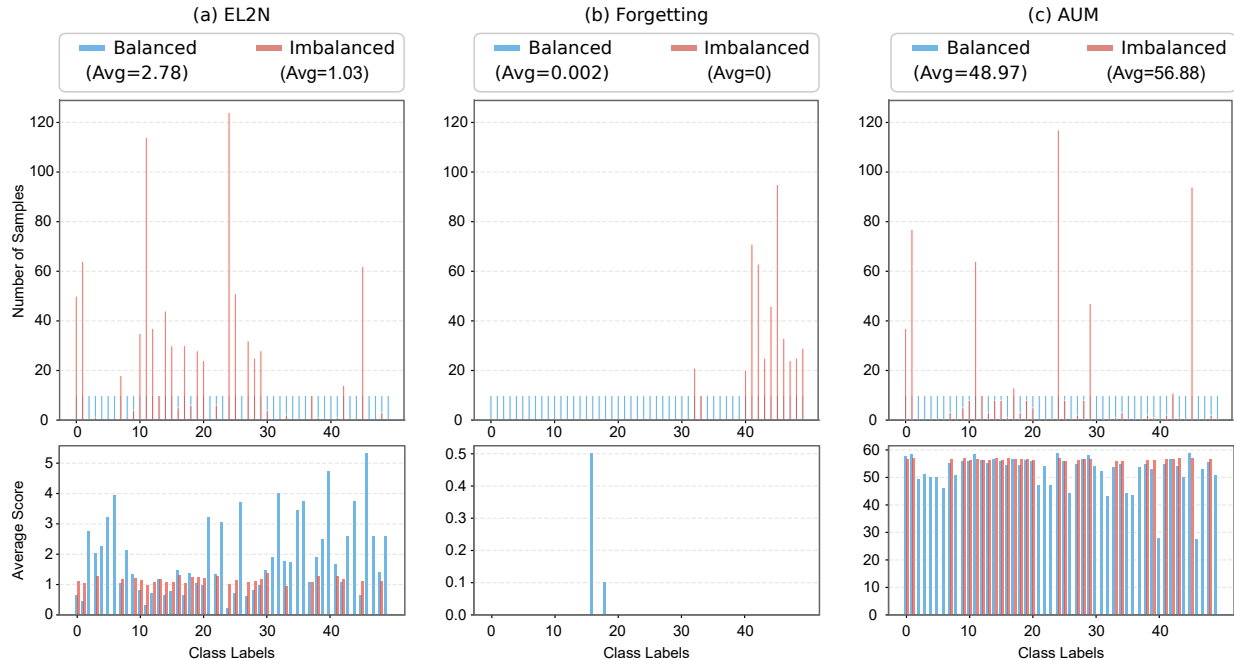


Figure 7: Sample and score distribution over class on both balanced and imbalanced cases. Top row: the sample distribution. Bottom row: the score distribution over class. For visualization purposes, only the first 50 classes are presented. IPC10 datasets are visualized and are selected from the “easiest” samples.

D.6. PCA with Different Pruning Methods.

Our PCA framework is designed to accommodate various pruning methods, and the results are summarized in Table 24. The experiments were conducted using a hard-label-only approach, with the AdamW optimizer. The standard deviation is computed from three independent runs.

We observed that EL2N (Paul et al., 2021) and AUM (Pleiss et al., 2020) consistently outperform the random baseline by a significant margin. Although AUM performs better than EL2N at IPC50 and IPC100, we chose EL2N as our baseline due to its efficiency, as EL2N utilizes training dynamics only during the early training phase (i.e., the first 10 epochs on the full dataset) while AUM requires full training (i.e., 90 epochs on the full dataset). A more detailed time breakdown can be found in Appendix D.8.

In contrast, Forgetting (Toneva et al., 2019) shows a substantial performance gap compared to EL2N and AUM; however, it still surpasses the random baseline across various IPC settings without introducing additional overheads. An explanation for the limitations of Forgetting is provided in Appendix D.4.

Table 24: PCA framework with different pruning methods.

IPC	Random	Forgetting	EL2N	AUM
10	4.6 \pm 0.1	8.6 \pm 0.2	22.8 \pm 0.3	21.9 \pm 0.3
50	20.6 \pm 0.1	24.1 \pm 0.4	39.1 \pm 0.2	39.2 \pm 0.1
100	31.7 \pm 0.6	36.2 \pm 0.3	45.5 \pm 0.4	46.4 \pm 0.2

D.7. Difference between Mosaic Augmentation

One approach similar to the “combining” process is Mosaic Augmentation, introduced in YOLOv4 (Bochkovskiy et al., 2020) for object detection tasks, as shown in Figure 8. However, the motivation behind it differs significantly. Combining images consolidates information from multiple sources into a single composite image, thereby saving storage space. In contrast, Mosaic Augmentation mixes multiple (i.e., four) images to facilitate the detection of objects outside their normal

context. Additionally, at the implementation level, Mosaic Augmentation loads four times as many images per given batch size, necessitating four times the storage. Nevertheless, the non-uniform combination method could potentially be leveraged in our “combining” approach, which we leave for future study.



Figure 8: Mosaic Augmentation. (Image directly taken from YOLOv4 (Bochkovski et al., 2020))

D.8. Computation Cost Analysis

One significant advantage of our PCA framework is its efficiency. Table 25 compares the costs associated with the traditional dataset compression framework, SRe²L, and our PCA method. Among the three stages of SRe²L, the “squeeze” stage is the most time-consuming, particularly when applied to ResNet with the entire ImageNet-1K dataset, which is quite resource-intensive. The parameter storage is 0.04 GB (44M). The second most time-consuming process is the “recover” stage. In contrast, the “relabel” process takes the least amount of time; however, it can become lengthy if the IPC is large due to the introduction of extensive labels, as noted by Xiao & He. A detailed breakdown of the timing is provided in Table 26. This table indicates that the I/O time, specifically the time required to save the labels, significantly contributes to the overall CPU time. This can be problematic for devices with limited CPU resources.

On the contrary, let us consider EL2N (Paul et al., 2021), which serves as an example in our primary experiments. The time of the “prune” process involves acquiring the training dynamics, which can be considerably shorter than training the entire model. Furthermore, since our approach is optimization-free, there are no additional costs incurred for combining the images, and we exclusively utilize hard labels instead of soft labels.

Table 25: Computation Cost of Dataset Compression between Traditional Framework and PCA. IPC-10, ImageNet-1K.

SRe ² L (Yin et al., 2023)	Squeeze	Recover	Relabel	PCA	Prune	Combine
Time ²	90 epochs	580 mins	33 mins	Time	10 epochs	-
Storage (GB)	0.04	0.15	5.67	Storage (GB)	-	0.15

Table 26: Relabel Cost Breakdown

Operation	CPU		GPU	
	Time (ms)	Memory (MB)	Time (ms)	Memory (MB)
Data Transfer to GPU	3.34	0.00	3.27	1,722.79
Mix Augmentation	0.45	22.74	0.21	0.00
Model Inference	4.48	0.00	30.07	9.17
Write to Disk	22.56	-13.60	0.12	0.00
Others (89 ops)	1.14	233.31	0.94	3,045.84

²All time data have been tested on a single RTX30390 GPU card.

E. Visualization

E.1. Visualization of Dataset Distillation Methods

Figure 9 visualizes the result of SRe²L (Yin et al., 2023). Figure 10 visualizes the result of CDA (Yin & Shen, 2024). Figure 11 visualizes the result of G-VBSM (Shao et al., 2024a). Figure 12 visualizes the result of LPLD (Xiao & He, 2024). Figure 13 visualizes the result of DWA (Du et al., 2024). Figure 14 visualizes the result of RDED (Sun et al., 2024). For all distillation methods (except for RDED; Sun et al. 2024), images undergo strong distortion.

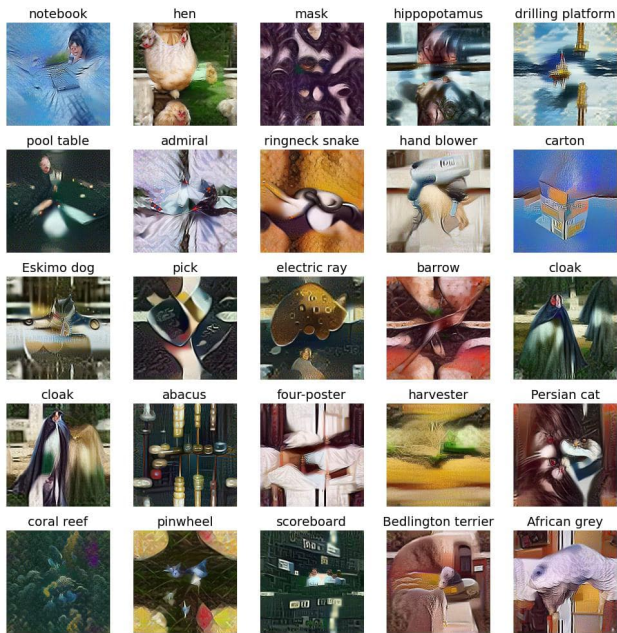


Figure 9: SRe²L (Yin et al., 2023)

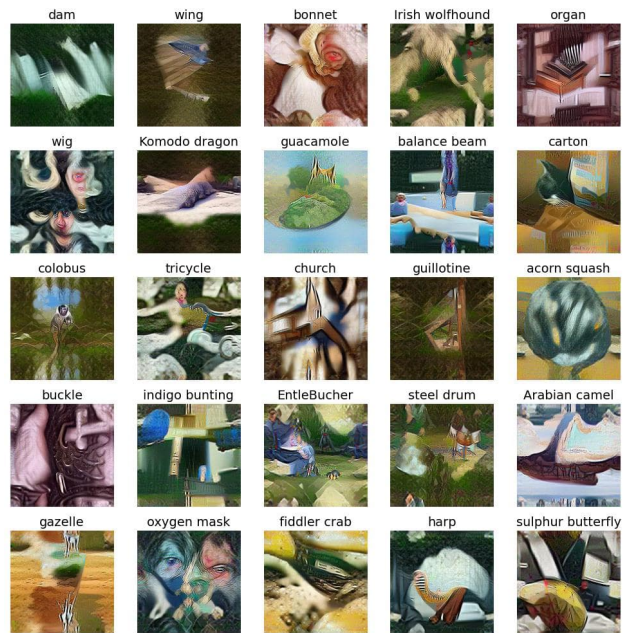


Figure 10: CDA (Yin & Shen, 2024)

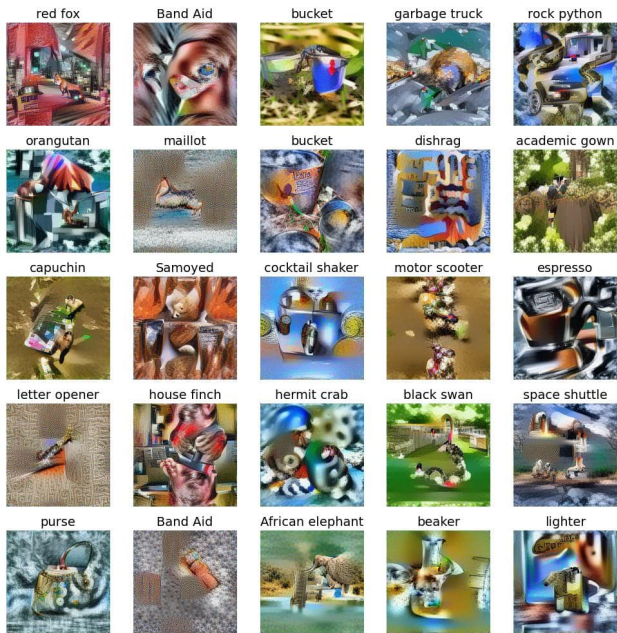


Figure 11: G-VBSM (Shao et al., 2024a)

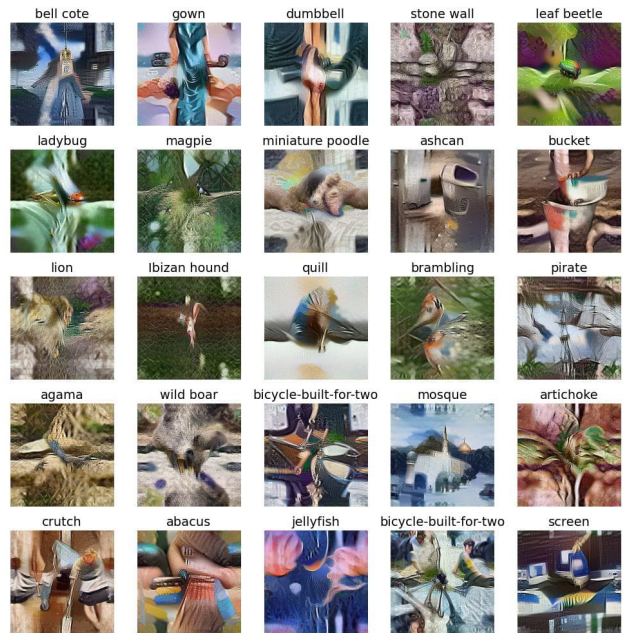


Figure 12: LPLD (Xiao & He, 2024)

Rethinking Large-scale Dataset Compression: Shifting Focus From Labels to Images

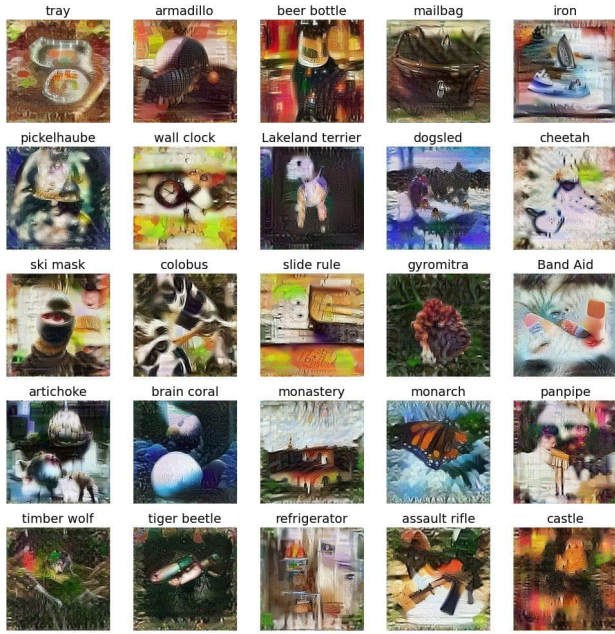


Figure 13: DWA (Du et al., 2024)

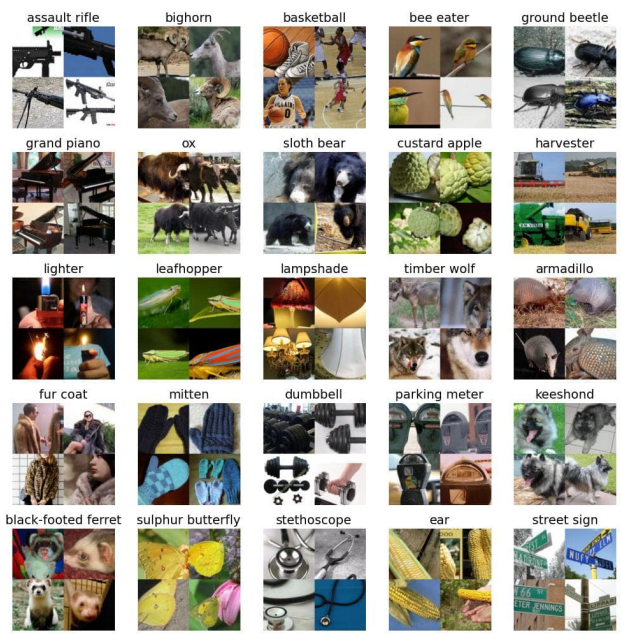


Figure 14: RDED (Sun et al., 2024)

E.2. Visualization of Dataset Pruning Methods

Figure 15 visualizes the result of Forgetting (Toneva et al., 2019). Figure 16 visualizes the result of AUM (Pleiss et al., 2020). Figure 17 visualizes the result of EL2N (Paul et al., 2021). Figure 18 visualizes the result of CCS (Zheng et al., 2023). The visualization results of all pruning methods followed the pruning rules, allowing for the clear observation that most of the selected images are distinct and visually easy to identify.

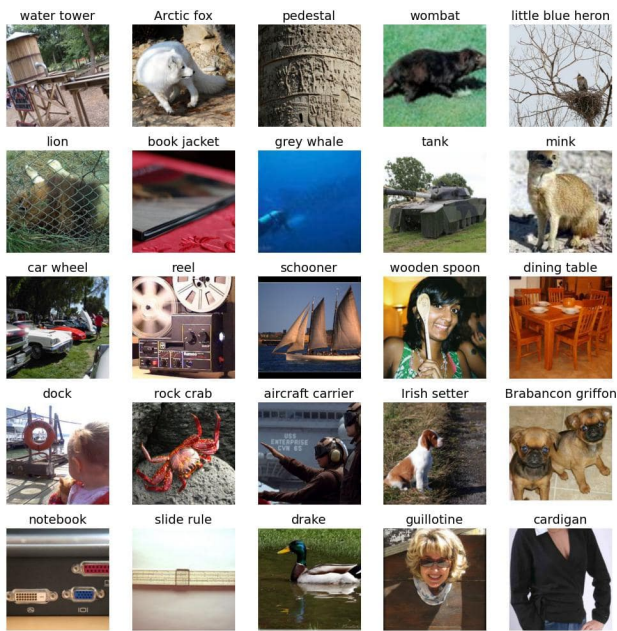


Figure 15: Forgetting (Toneva et al., 2019)

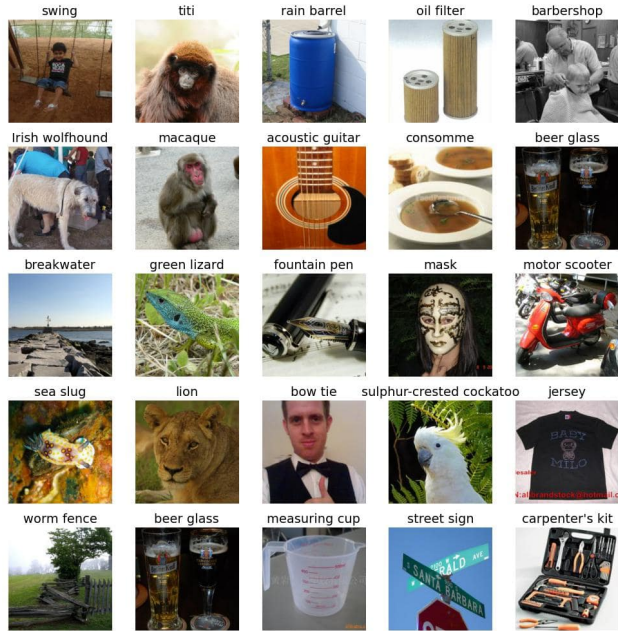


Figure 16: AUM (Pleiss et al., 2020)

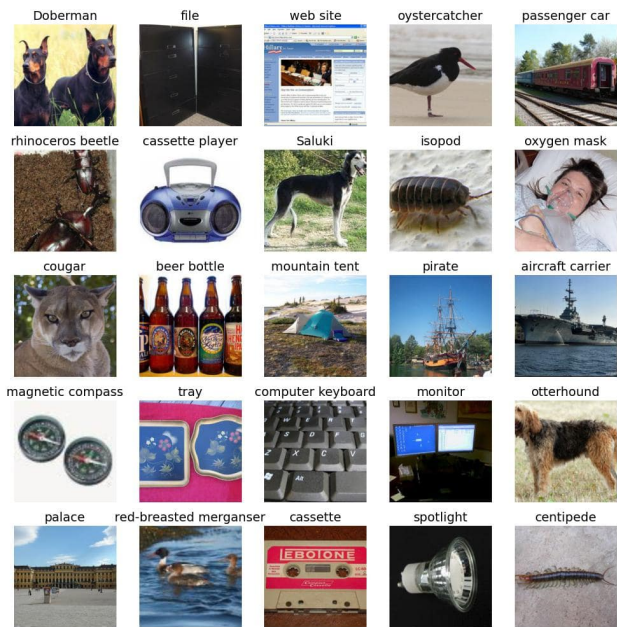


Figure 17: EL2N (Paul et al., 2021)

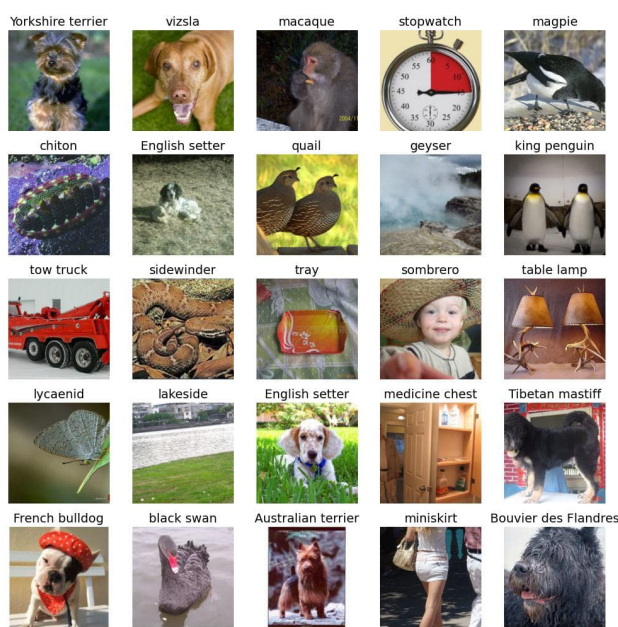


Figure 18: CCS (Zheng et al., 2023)

E.3. Visualization of PCA

Figure 19 shows the images of our PCA framework which uses EL2N (Paul et al., 2021) as the selection metric. Even when adhering to pruning rules, the cobined images may not appear visually similar. For example, the "sax" class (first row, second column) demonstrates distinct contexts (i.e., placing the sax on a purple background or a musician playing the sax). This further demonstrates the importance of scaling-law aware augmentation, as inappropriate subsequent training augmentations can lead to a significant difficulty increase in the images.

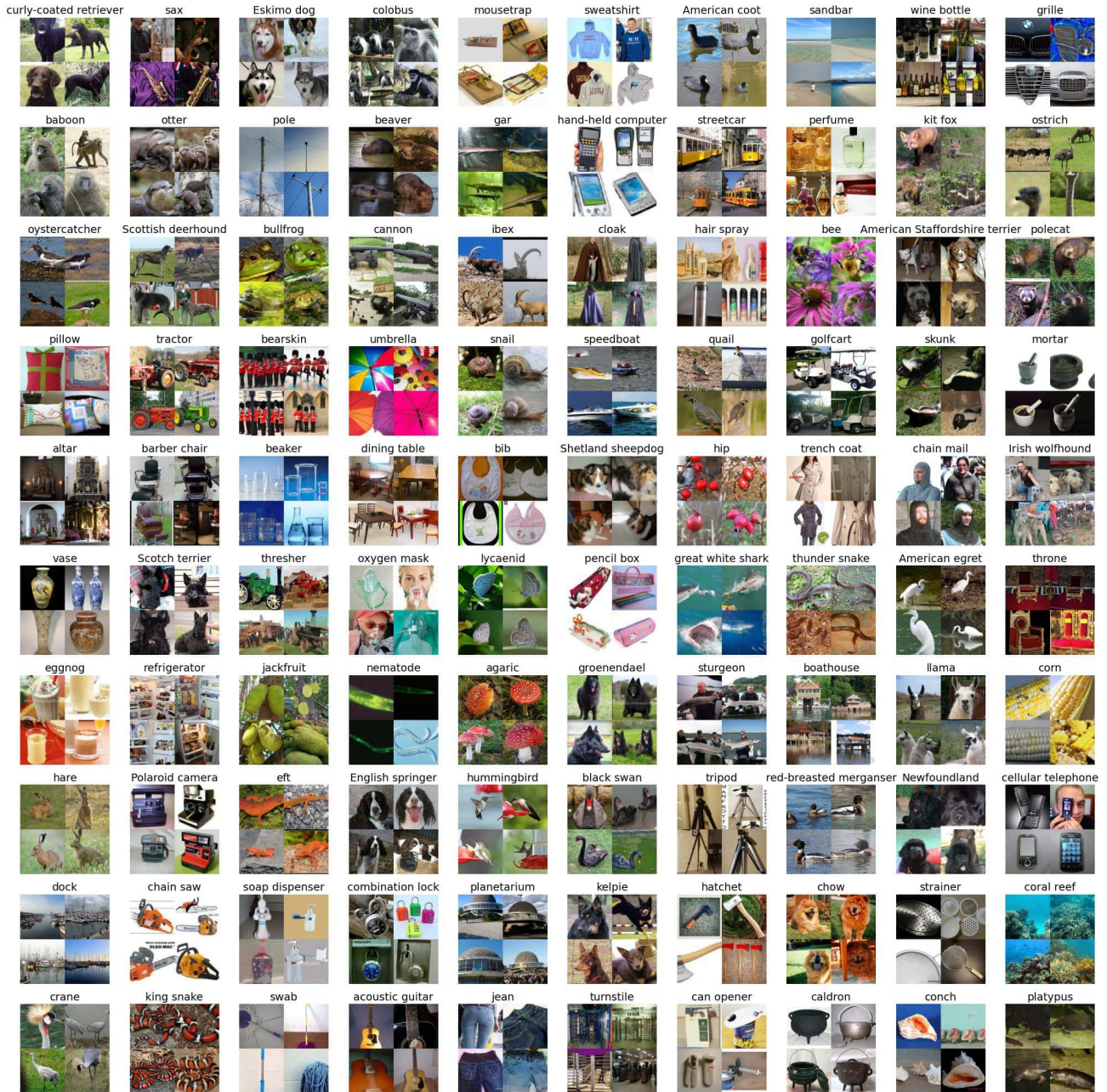


Figure 19: Ours (PCA based on EL2N).

F. Limitation

Our augmentation procedures, including patch extraction, are heuristically designed. While they demonstrate strong empirical effectiveness, their optimality is not theoretically guaranteed.

G. Future Work

Given that the proposed PCA functions as a framework, there is potential to explore **different choices** of the modules, such as pruning metrics, combining strategies, and specific augmentation methods. It is notable that pruning can extend beyond the original dataset. Instead of only developing new pruning metrics, one could target different datasets. In this paper, the primary reason for pruning on the original dataset is that most existing dataset distillation methods do not outperform random baselines, indicating that original images are sufficiently effective. Hence, there is **significant value** in considering pruning on potentially high-performing distilled datasets (e.g., YOCO; He et al. 2024) or on generated datasets (e.g., diffusion-based DD methods; Su et al. 2024). Beyond accuracy, future frameworks might also jointly optimize additional metrics, such as robustness, fairness, or interpretability, while maintaining the same compressed dataset constraint.